

## Research Article

Table 1. Baseline characteristics of all patients, and patients assigned to the model building or validation groups.

	All patients n = 496	Model group n = 331	Validation group n = 165
Gender: male	250 (50%)	170 (51%)	80 (48%)
Age (years)	57.1 ± 9.9	56.8 ± 9.7	57.5 ± 10.2
ALT (IU/L)	78.6 ± 60.8	78.1 ± 61.4	79.7 ± 59.6
GGT (IU/L)	59.3 ± 63.6	58.9 ± 62.0	60.2 ± 66.9
Platelets (10 <sup>9</sup> /L)	154 ± 53	153 ± 52	154 ± 56
Fibrosis: F3-4	121 (24%)	80 (24%)	41 (25%)
HCV-RNA: >600,000 IU/ml	409 (82%)	273 (82%)	136 (82%)
ISDR mutation: ≤1	220 (88%)	290 (88%)	145 (88%)
Core 70 (Arg/Gln or His)	293 (59%)/203 (41%)	197 (60%)/134 (40%)	96 (58%)/69 (42%)
Core 91 (Leu/Met)	299 (60%)/197 (40%)	200 (60%)/131 (40%)	99 (60%)/66 (40%)
<i>IL28B</i> : Minor allele	151 (30%)	101 (31%)	50 (30%)
SVR	194 (39%)	129 (39%)	65 (39%)
Relapse	152 (31%)	103 (31%)	49 (30%)
NVR	150 (30%)	99 (30%)	51 (31%)

ALT, alanine aminotransferase; GGT, gamma-glutamyltransferase; ISDR, interferon sensitivity determining region; Arg, arginine; Gln, glutamine; His, histidine; Leu, leucine; Met, methionine; Minor, heterozygote or homozygote of minor allele; SVR, sustained virological response; NVR, null virological response.

Japanese [6], European [7], and a multi-ethnic population [8,9]. The last three studies focused on the association of SNPs in the *IL28B* region with SVR [7–9] but we found a stronger association with NVR [6]. In addition to these host genetic factors, we have reported that mutations within a stretch of 40 amino acids in the NS5A region of HCV, designated as the IFN sensitivity determining region (ISDR), are closely associated with the virological response to IFN therapy: a lower number of mutations is associated with treatment failure [10–13]. Amino acid substitutions at positions 70 and 91 of the HCV core region (Core70, Core91) also have been reported to be associated with response to PEG-IFN/RBV therapy: glutamine (Gln) or histidine (His) at Core70 and methionine (Met) at Core91 are associated with treatment resistance [4,14]. The importance of substitutions in the HCV core and ISDR was confirmed recently by a Japanese multicenter study [15]. How these viral factors contribute to response to therapy is yet to be determined. For general application in clinical practice, host genetic factors and viral factors should be considered together.

Data mining analysis is a family of non-parametric regression methods for predictive modeling. Software is used to automatically explore the data to search for optimal split variables and to build a decision tree structure [16]. The major advantage of decision tree analysis over logistic regression analysis is that the results of the analysis are presented in the form of flow chart, which can be interpreted intuitively and readily made available for use in clinical practice [17]. The decision tree analysis has been utilized to define prognostic factors in various diseases [18–25]. We have reported recently its usefulness for the prediction of an early virological response (undetectable HCV-RNA within 12 weeks of therapy) to PEG-IFN/RBV therapy in chronic hepatitis C [26].

This study aimed to define the pre-treatment prediction of response to PEG-IFN/RBV therapy through the integrated analysis of host factors, such as the *IL28B* genetic polymorphism and various clinical covariates, as well as viral factors, such as mutations in the HCV core and ISDR and serum HCV-RNA load. In addition,

for the general application of these results in clinical practice, decision models for the pre-treatment prediction of response were determined by data mining analysis.

## Materials and methods

### Patients

This was a multicentre retrospective study supported by the Japanese Ministry of Health, Labor and Welfare. Data were collected from a total of 496 chronic hepatitis C patients who were treated with PEG-IFN alpha and RBV at five hospitals and universities throughout Japan. Of these, 98 patients also were included in the original GWAS analysis [6]. The inclusion criteria in this study were as follows (1) infection by genotype 1b, (2) lack of co-infection with hepatitis B virus or human immunodeficiency virus, (3) lack of other causes of liver disease, such as autoimmune hepatitis, and primary biliary cirrhosis, (4) completion of at least 24 weeks of therapy, (5) adherence of more than 80% to the planned dose of PEG-IFN and RBV for the NVR patients, (6) availability of DNA for the analysis of the genetic polymorphism of *IL28B*, and (7) availability of serum for the determination of mutations in the ISDR and substitutions of Core70 and Core91 of HCV. Patients received PEG-IFN alpha-2a (180 µg) or 2b (1.5 µg/kg) subcutaneously every week and were administered a weight adjusted dose of RBV (600 mg for <60 kg, 800 mg for 60–80 kg, and 1000 mg for >80 kg daily) which is the recommended dosage in Japan. Written informed consent was obtained from each patient and the study protocol conformed to the ethical guidelines of the Declaration of Helsinki and was approved by the institutional ethics review committee. The baseline characteristics are listed in Table 1. For the data mining analysis, 67% of the patients (331 patients) were assigned randomly to the model building group and 33% (165 patients) to the validation group. There were no significant differences in the clinical backgrounds between these two groups.

### Laboratory and histological tests

Blood samples were obtained before therapy and were analyzed for hematologic tests and for blood chemistry and HCV-RNA. Sequences of ISDR and the core region of HCV were determined by direct sequencing after amplification by reverse-transcription and polymerase chain reaction as reported previously [4,11]. Genetic polymorphism in one tagging SNP located near the *IL28B* gene (rs8099917) was determined by the GWAS or DigiTag2 assay [27]. Homozygosity (GG) or heterozygosity (TG) of the minor sequence was defined as having the *IL28B* minor allele, whereas homozygosity for the major sequence (TT) was

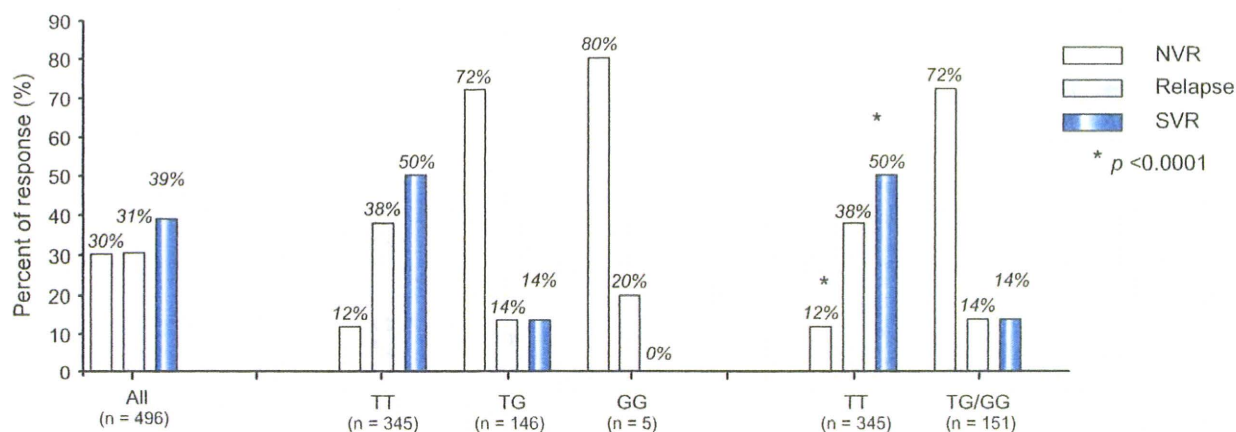


**Fig. 1. Association between the *IL28B* genotype (rs8099917) and treatment response.** The rates of response to treatment are shown for each rs8099917 genotype. The rate of null virological response (NVR), relapse, and sustained virological response (SVR) is shown. The *p* values are from Fisher's exact test. The rate of NVR was significantly higher ( $p < 0.0001$ ) and the rate of SVR was significantly lower ( $p < 0.0001$ ) in patients with the *IL28B* minor allele compared to those with the major allele. [This figure appears in colour on the web.]

defined as having the *IL28B* major allele. In this study, NVR was defined as a less than 2 log reduction of HCV-RNA at week 12 and detectable HCV-RNA by qualitative PCR with a lower detection limit of 50 IU/ml (Amplicor, Roche Diagnostic systems, CA) at week 24 during therapy. RVR (rapid virological response) and complete early virological response (cEVR) were defined as undetectable HCV-RNA at 4 weeks and 12 weeks during therapy and SVR was defined as undetectable HCV-RNA 24 weeks after the completion of therapy. Relapse was defined as reappearance of HCV-RNA after the completion of therapy. The stage of liver fibrosis was scored according to the METAVIR scoring system: F0 (no fibrosis), F1 (mild fibrosis: portal fibrosis without septa), F2 (moderate fibrosis: few septa), F3 (severe fibrosis: numerous septa without cirrhosis) and F4 (cirrhosis). Percentage of steatosis was quantified in 111 patients by determining the average proportion of hepatocytes affected by steatosis.

#### Statistical analysis

Associations between pre-treatment variables and treatment response were analyzed by univariate and multivariate logistic regression analysis. Associations between the *IL28B* polymorphism and sequences of HCV were analyzed by Fisher's exact test. SPSS software v.15.0 (SPSS Inc., Chicago, IL) was used for these analyses. For the data mining analysis, IBM-SPSS Modeler version 13.0 (IBM-SPSS Inc., Chicago, IL) software was utilized as reported previously [26]. The patients used for model building were divided into two groups at each step of the analysis based on split variables. Each value of each variable was considered as a potential split. The optimum variables and cut-off values were determined by a statistical search algorithm to generate the most significant division into two prognostic subgroups that were as homogeneous as possible for the probability of SVR. Thereafter, each subgroup was evaluated again and divided further into subgroups. This procedure was repeated until no additional significant variable was detected or the sample size was below 15. To avoid over-fitting, 10-fold cross validation was used in the tree building process. The reproducibility of the resulting model was tested with the data from the validation patients.

## Results

### Association between the *IL28B* (rs8099917) genotype and the PEG-IFN/RBV response

The rs8099917 allele frequency was 70% for TT ( $n = 345$ ), 29% for TG ( $n = 146$ ), and 1% for GG ( $n = 5$ ). We defined the *IL28B* major allele as homozygous for the major sequence (TT) and the *IL28B* minor allele as homozygous (GG) or heterozygous (TG) for the minor sequence. The rate of NVR was significantly higher (72% vs. 12%,  $p < 0.0001$ ) and the rate of SVR was significantly lower (14% vs. 50%,  $p < 0.0001$ ) in patients with the *IL28B* minor allele compared to those with the major allele (Fig. 1).

### Effect of the *IL28B* polymorphism, substitutions in the ISDR, Core70, and Core91 of HCV on time-dependent clearance of HCV

Patients were stratified according to their *IL28B* allele type, the number of mutations in the ISDR, the amino acid substitutions in Core70 and Core91, and the rate of undetectable HCV-RNA at 4, 8, 12, 24, and 48 weeks after the start of therapy was analyzed (Fig. 2A–D). The rate of undetectable HCV-RNA was significantly higher in patients with the *IL28B* major allele than the minor allele, in patients with two or more mutations in the ISDR compared to none or only one mutation, in patients with arginine (Arg) at Core70 rather than Gln/His, and in patients with leucine (Leu) at Core91 rather than Met. The difference was most significant when stratified by the *IL28B* allele type. The rate of RVR and cEVR was significantly more frequent in patients with the *IL28B* major allele compared to those with the *IL28B* minor allele: 9% vs. 3% for RVR ( $p < 0.005$ ) and 57% vs. 11% for cEVR ( $p < 0.0001$ ). These findings suggest that *IL28B* has the greatest impact on early virological response to therapy.

### Association between substitutions in the ISDR and relapse after the completion of therapy

Patients were stratified according to the *IL28B* allele, number of mutations in the ISDR, and amino acid substitutions of Core70 and Core91, and the rate of relapse was analyzed (Fig. 3A and B). Among patients who achieved cEVR, the rate of relapse was significantly lower in patients with two or more mutations in the ISDR compared to those with only one or no mutations (15% vs. 31%,  $p < 0.005$ ) (Fig. 3B). On the other hand, the relapse rate was not different between the *IL28B* major and minor alleles within patients who achieved RVR (3% vs. 0%) or cEVR (28% vs. 29%) (Fig. 3A). Amino acid substitutions of Core70 and Core91 were not associated with the rate of relapse (data not shown).

### Factors associated with response by multivariate logistic regression analysis

By univariate analysis, the minor allele of *IL28B* ( $p < 0.0001$ ), one or no mutations in the ISDR ( $p = 0.03$ ), high serum level of

## Research Article

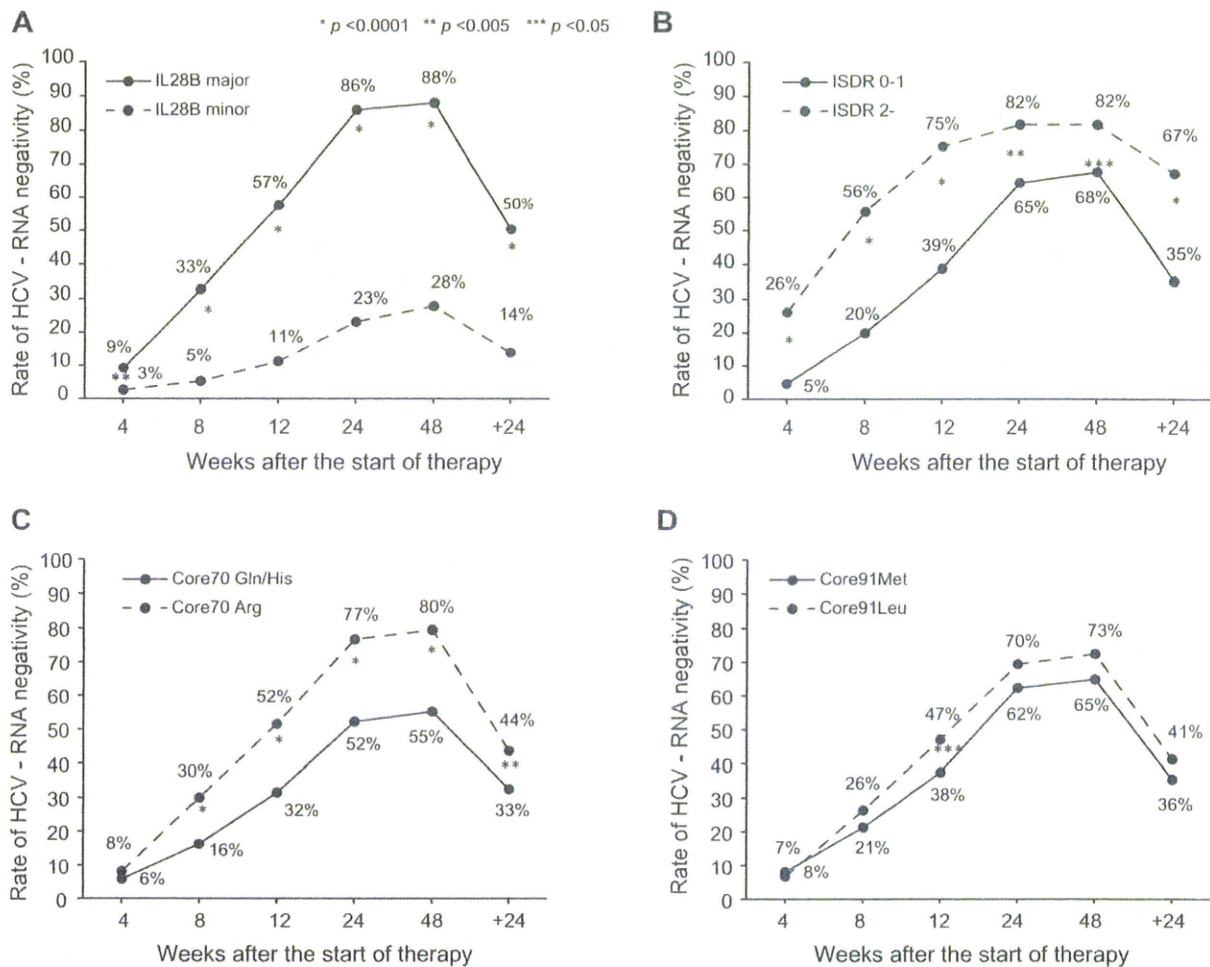


**Fig. 2. Effect of *IL28B* mutations in the ISDR, Core70 and Core91 of HCV on time-dependent clearance of HCV.** The rate of undetectable HCV-RNA was plotted for serial time points after the start of therapy (4, 8, 12, 24, and 48 weeks) and for 24 weeks after the completion of therapy. Patients were stratified according to (A) the *IL28B* allele (minor allele vs. major allele), (B) the number of mutations in the ISDR (0-1 mutation vs. 2 or more mutations), amino acid substitutions of (C) Core70 (Gln/His vs. Arg), and (D) Core91 (Met vs. Leu). The *p* values are from Fisher's exact test.

HCV-RNA ( $p = 0.035$ ), Gln or His at Core70 ( $p < 0.0001$ ), low platelet counts ( $p = 0.009$ ), and advanced fibrosis ( $p = 0.0002$ ) were associated with NVR. By multivariate analysis, the minor allele of *IL28B* (OR = 20.83, 95%CI = 11.63–37.04,  $p < 0.0001$ ) was associated with NVR independent of other covariates (Table 2). Notably, mutations in the ISDR ( $p = 0.707$ ) and at amino acid Core70 ( $p = 0.207$ ) were not significant in multivariate analysis due to the positive correlation with the *IL28B* polymorphism ( $p = 0.004$  for ISDR and  $p < 0.0001$  for Core70, Fig. 4).

Genetic polymorphism of *IL28B* also was associated with SVR (OR = 7.41, 95% CI = 4.05–13.57,  $p < 0.0001$ ) independent of other covariates, such as platelet counts, fibrosis, and serum levels of HCV-RNA. Mutation in the ISDR was an independent predictor of SVR (OR = 2.11, 95% CI = 1.06–4.18,  $p = 0.033$ ) but the amino acid at Core70 was not (Table 3).

### Factors associated with the *IL28B* polymorphism

Patients with the *IL28B* minor allele had significantly higher serum level of gamma-glutamyltransferase (GGT) and a higher

frequency of hepatic steatosis (Table 4). When the association between the *IL28B* polymorphism and HCV sequences was analyzed, Gln or His at Core70, that is linked to resistance to PEG-IFN and RBV therapy [4,14,15], was significantly more frequent in patients with the minor *IL28B* allele than in those with the major allele (67% vs. 30%,  $p < 0.0001$ ) (Fig. 4). Other HCV sequences with an IFN resistant phenotype also were more prevalent in patients with the minor *IL28B* allele than those with the major allele: Met at Core91 (46% vs. 37%,  $p = 0.047$ ) and one or no mutations in the ISDR (94% vs. 85%,  $p = 0.004$ ) (Fig. 4).

### Data mining analysis

Data mining analysis was performed to build a model for the prediction of SVR and the result is shown in Fig. 5. The analysis selected four predictive variables, resulting in six subgroups of patients. Genetic polymorphism of *IL28B* was selected as the best predictor of SVR. Patients with the minor *IL28B* allele had a lower probability of SVR and a higher probability of NVR than those with the major *IL28B* allele (SVR: 14% vs. 50%, NVR: 72% vs.

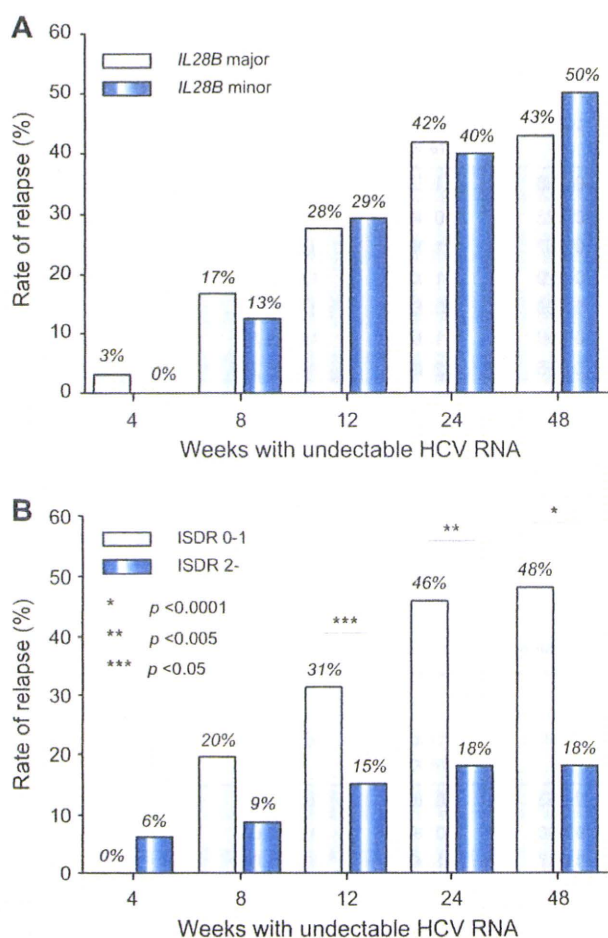


**Fig. 3. Association between relapse and the *IL28B* allele or mutations in the ISDR.** The rate of relapse was calculated for patients who had undetectable HCV-RNA at serial time points after the start of therapy (4, 8, 12, 24, and 48 weeks). Patients were stratified according to (A) the *IL28B* allele (minor allele vs. major allele) and (B) the number of mutations in the ISDR (0–1 mutation vs. 2 or more mutations). The *p* values are from Fisher's exact test. [This figure appears in colour on the web.]

12%). After stratification by the *IL28B* allele, patients with low platelet counts ( $<140 \times 10^9/L$ ) had a lower probability of SVR and higher probability of NVR than those with high platelet counts ( $\geq 140 \times 10^9/L$ ): for the minor *IL28B* allele, SVR was 7% vs. 19%, and NVR was 84% vs. 62%, and for the major *IL28B* allele, SVR was 32% vs. 66% and NVR was 16% vs. 8%. Among patients with the major *IL28B* allele and low platelet counts, those with two or more mutations in the ISDR had a higher probability of SVR and lower probability of relapse than those with one or no mutations in the ISDR (SVR: 75% vs. 27%, and relapse: 8% vs. 57%). Among patients with the major *IL28B* allele and high platelet counts, those with a low HCV-RNA titer ( $<600,000$  IU/ml) had a higher probability of SVR and lower probability of NVR and relapse than those with a high HCV-RNA titer (SVR: 90% vs. 61%, NVR: 0% vs. 10%, and relapse: 10% vs. 29%). The sensitivity and specificity of the decision tree were 78% and 70%, respectively. The area under the receiver operating characteristic (ROC) curve of the model was 0.782 (data not shown). The pro-

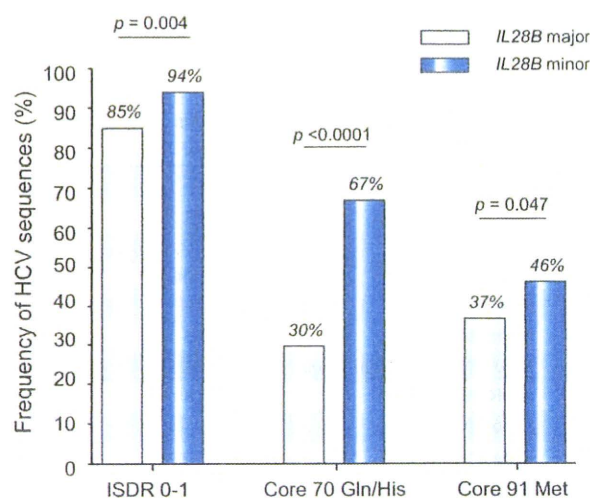


**Fig. 4. Associations between the *IL28B* allele and HCV sequences.** The prevalence of HCV sequences predicting a resistant phenotype to IFN was higher in patients with the minor *IL28B* allele than those with major allele. (A) 0 or 1 mutation in the ISDR of NS5A, (B) Gln or His at Core70, and (C) Met at Core91. *p* values are from Fisher's exact test. [This figure appears in colour on the web.]

portion of patients with advanced fibrosis (F3–4) was 39% (84/217) in patients with low platelet counts ( $<140 \times 10^9/L$ ) compared to 13% (37/279) in those with high platelet counts ( $\geq 140 \times 10^9/L$ ).

#### Validation of the data mining analysis

The results of the data mining analysis were validated with 165 patients who differed from those used for model building. Each patient was allocated to one of the six subgroups for the validation using the flow-chart form of the decision tree. The rate of SVR and NVR in each subgroup was calculated. The rates of SVR and NVR for each subgroup of patients were closely correlated between the model building and the validation patients ( $r^2 = 0.99$  and  $0.98$ ) (Fig. 6).

#### Discussion

The rate of NVR after 48 weeks of PEG-IFN/RBV therapy among patients infected with HCV of genotype 1 is around 20–30%. Previously, there have been no reliable baseline predictors of NVR or SVR. Because more potent therapies, such as protease and polymerase inhibitor of HCV [28,29] and nitazoxanide [30], are in clinical trials and may become available in the near future, a pre-treatment prediction of the likelihood of response may be helpful for patients and physicians, to support clinical decisions about whether to begin the current standard of care or whether to wait for emerging therapies. This study revealed that the *IL28B* polymorphism was the overwhelming predictor of NVR and is independent of host factors and viral sequences reported previously. The *IL28B* encodes a protein also known as IFN-lambda 3, which is thought to suppress the replication of various viruses including HCV [31,32]. The results of the current study and the findings of the GWAS studies [6–9] may provide the rationale for developing diagnostic testing or an IFN-lambda based therapy for chronic hepatitis C in the future.

## Research Article

Table 2. Factors associated with NVR analyzed by univariate and multivariate logistic regression analysis.

	Univariate			Multivariate		
	Odds ratio	95%CI	p value	Odds ratio	95%CI	p value
Gender: female	0.98	0.67-1.45	0.938	1.29	0.75-2.23	0.363
Age	1.01	0.97-1.01	0.223	0.99	0.97-1.02	0.679
ALT	1.00	1.00-1.00	0.867	1.00	0.99-1.00	0.580
GGT	1.004	1.00-1.01	0.029	1.00	1.00-1.00	0.715
Platelets	0.95	0.91-0.99	0.009	0.92	0.87-0.98	0.006
Fibrosis: F3-4	2.23	1.46-3.42	0.0002	1.97	1.09-3.57	0.025
HCV-RNA: $\geq 600,000$ IU/ml	1.83	1.05-3.19	0.035	2.49	1.17-5.29	0.018
ISDR mutation: $\leq 1$	2.14	1.08-4.22	0.030	0.96	0.78-1.18	0.707
Core 70 (Gln/His)	3.23	2.16-4.78	<0.0001	1.41	0.83-2.42	0.207
Core 91 (Met)	1.39	0.95-2.06	0.093	1.21	0.72-2.04	0.462
IL28B: Minor allele	19.24	11.87-31.18	<0.0001	20.83	11.63-37.04	<0.0001

ALT, alanine aminotransferase; GGT, gamma-glutamyltransferase; ISDR, interferon sensitivity determining region; Gln, glutamine; His, histidine; Met, methionine; Minor allele, heterozygote or homozygote of minor allele.

Table 3. Factors associated with SVR analyzed by univariate and multivariate logistic regression analysis.

	Univariate			Multivariate		
	Odds ratio	95%CI	p value	Odds ratio	95%CI	p value
Gender: female	0.81	0.56-1.16	0.253	0.86	0.55-1.35	0.508
Age	0.97	0.95-0.99	0.0003	0.99	0.96-1.01	0.199
ALT	1.00	1.00-1.00	0.337	1.00	1.00-1.01	0.108
GGT	1.00	1.00-1.00	0.273	1.00	1.00-1.00	0.797
Platelets	1.12	1.01-1.16	<0.0001	1.13	1.08-1.19	<0.0001
Fibrosis: F0-2	2.64	1.65-4.22	<0.0001	1.87	1.07-3.28	0.029
HCV-RNA: <600,000 IU/ml	2.49	1.55-3.98	0.0001	2.75	1.55-4.90	0.001
ISDR mutation: $\leq 2$	3.78	2.14-6.68	<0.0001	2.11	1.06-4.18	0.033
Core 70 (Arg)	1.61	1.11-2.28	0.012	0.84	0.52-1.35	0.470
Core 91 (Leu)	1.28	0.88-1.85	0.185	1.26	0.81-1.96	0.300
IL28B: Major allele	6.21	3.75-10.31	<0.0001	7.41	4.05-13.57	<0.0001

ALT, alanine aminotransferase; GGT, Gamma-glutamyltransferase; ISDR, interferon sensitivity determining region; Arg, arginine; Leu, leucine; Major allele, homozygote of major allele.

Among baseline factors, IL28B was the most significant predictor of NVR and SVR. Moreover, the IL28B allele type was also correlated with early virological response: the rate of RVR and cEVR was significantly high for the IL28B major allele compared to the IL28B minor allele: 9% vs. 3% for RVR and 57% vs. 11% for cEVR (Fig. 2). On the other hand, the relapse rate was not different between the IL28B genotypes within patients who achieved RVR or cEVR (Fig. 3). We believe that optimal therapy should be based on baseline features and a response-guided approach. Our findings suggest that the IL28B genotype is a useful baseline predictor of virological response which should be used for selecting the treatment regimen: whether to treat patients with PEG-IFN and RBV or to wait for more effective future therapy including direct acting antiviral drugs. On the other hand, baseline IL28B genotype might not be suitable for determining the treatment duration in patients who started PEG-IFN/RBV therapy

and whose virological response is determined because the IL28B genotype is not useful for the prediction of relapse. The duration of therapy should be personalized based on the virological response. Future studies need to explore whether the combination of baseline IL28B genotype and response-guided approach further improves the optimization of treatment duration.

The SVR rate in patients having the IL28B minor allele was 14% in the present study while it was 23% in Caucasians and 9% in African Americans in a study by McCarthy et al. [33]. On the other hand, the SVR rate in patients having the IL28B minor allele was 28% in genotypes 1/4 compared to 80% in genotypes 2/3 in a study by Rauch et al. [9]. These data imply that the impact of the IL28B polymorphism on response to therapy may be different in terms of race, geographical areas, or HCV genotypes, and that our data need to be validated in future studies including different populations and geographical areas before generalization.

Table 4. Factors associated with IL28B genotype.

	IL28B major allele n = 345	IL28B minor allele n = 151	p value
Gender: male	166 (48%)	84 (56%)	0.143
Age (years)	57 ± 10	57 ± 10	0.585
ALT (IU/L)	79 ± 60	78 ± 62	0.842
Platelets (10 <sup>9</sup> /L)	153 ± 54	155 ± 52	0.761
GGT (IU/L)	51 ± 45	78 ± 91	0.001
Fibrosis: F3-4	76 (22%)	45 (30%)	0.063
Steatosis:			
>10%	16/88 (18%)	13/23 (57%)	0.024
>30%	6/88 (7%)	6/23 (26%)	0.017
HCV-RNA: >600,000 IU/ml	284 (82%)	125 (83%)	1.000

ALT, alanine aminotransferase; GGT, gamma-glutamyltransferase.

Four GWAS studies have shown the association between a genetic polymorphism near the IL28B gene and response to PEG-IFN plus RBV therapy. The SNPs that showed significant association with response were rs12979860 [8] and rs8099917 [6,7,9]. There is a strong linkage-disequilibrium (LD) between these two SNPs as well as several other SNPs near the IL28B gene in Japanese patients [34] but the degree of LD was weaker in Caucasians and Hispanics [8]. Thus, the combination of SNPs is not useful for predicting response in Japanese patients but may improve the predictive value in patients other than Japanese who have weaker LD between SNPs.

Other significant predictors of response independent of IL28B genotype were platelet counts, stage of fibrosis, and HCV RVA load. A previous study reported that platelet count is a predictor of response to therapy [35], and the lower platelet count was related with advanced liver fibrosis in the present study. The association between response to therapy and advanced fibrosis independent of the IL28B polymorphism is consistent with a recent study by Rauch et al. [9].

There is agreement that the viral genotype is significantly associated with the treatment outcome. Moreover, viral factors such as substitutions in the ISDR of the NS5A region [10] or in the amino acid sequence of the HCV core [4] have been studied in relation to the response to IFN treatment. The amino acid Gln or His at Core70 and Met at Core91 are repeatedly reported to be associated with resistance to therapy [4,14,15] in Japanese patients but these data wait to be validated in different populations or other geographical areas. In this study, we confirmed that patients with two or more mutations in the ISDR had a higher rate of undetectable HCV-RNA at each time point during therapy. In addition, the rate of relapse among patients who achieved cEVR was significantly lower in patients with two or more mutations in ISDR compared to those with only one or no mutations (15% vs. 31%,  $p < 0.05$ ). Thus, the ISDR sequence may be used to predict a relapse among patients who achieved virological response during therapy, while the IL28B polymorphism may be used to predict the virological response before therapy. A higher number of mutations in the ISDR are reported to have close association with SVR in Japanese [11-13,15,36] or Asian [37,38] populations but data from Western countries have been controversial [39-42]. A meta-analysis of 1230 patients including 525 patients from Europe has shown that there was a positive

correlation between the SVR and the number of mutations in the ISDR in Japanese as well as in European patients [43] but this correlation was more pronounced in Japanese patients. Thus, geographical factors may account for the different impact of ISDR on treatment response, which may be a potential limitation of our study.

To our surprise, these HCV sequences were associated with the IL28B genotype: HCV sequences with an IFN resistant phenotype were more prevalent in patients with the minor IL28B allele than those with the major allele. This was an unexpected finding, as we initially thought that host genetics and viral sequences were completely independent. A recent study reported that the IL28B polymorphism (rs12979860) was significantly associated with HCV genotype: the IL28B minor allele was more frequent in HCV genotype 1-infected patients compared to patients infected with HCV genotype 2 or 3 [33]. Again, patients with the IL28B minor allele (IFN resistant genotype) were infected with HCV sequences that are linked to an IFN resistant phenotype. The mechanism for this association is unclear, but may be related to an interaction between the IL28B genotype and HCV sequences in the development of chronic HCV infection as discussed by McCarthy et al., since the IL28B polymorphism was associated with the natural clearance of HCV [44]. Alternatively, the HCV sequence within the patient may be selected during the course of chronic infection [45,46]. These hypotheses should be explored through prospective studies of spontaneous HCV clearance or by testing the time-dependent changes in the HCV sequence during the course of chronic infection.

How these host and viral factors can be integrated to predict the response to therapy in future clinical practice is an important question. Because various host and viral factors interact in the same patient, predictive analysis should consider these factors in combination. Using the data mining analysis, we constructed a simple decision tree model for the pre-treatment prediction of SVR and NVR to PEG-IFN/RBV therapy. The classification of patients based on the genetic polymorphism of IL28B, mutation in the ISDR, serum levels of HCV-RNA, and platelet counts, identified subgroups of patients who have the lowest probabilities of NVR (0%) with the highest probabilities of SVR (90%) as well as those who have the highest probabilities of NVR (84%) with the lowest probability of SVR (7%). The reproducibility of the model was confirmed by the independent validation based on a second

Research Article

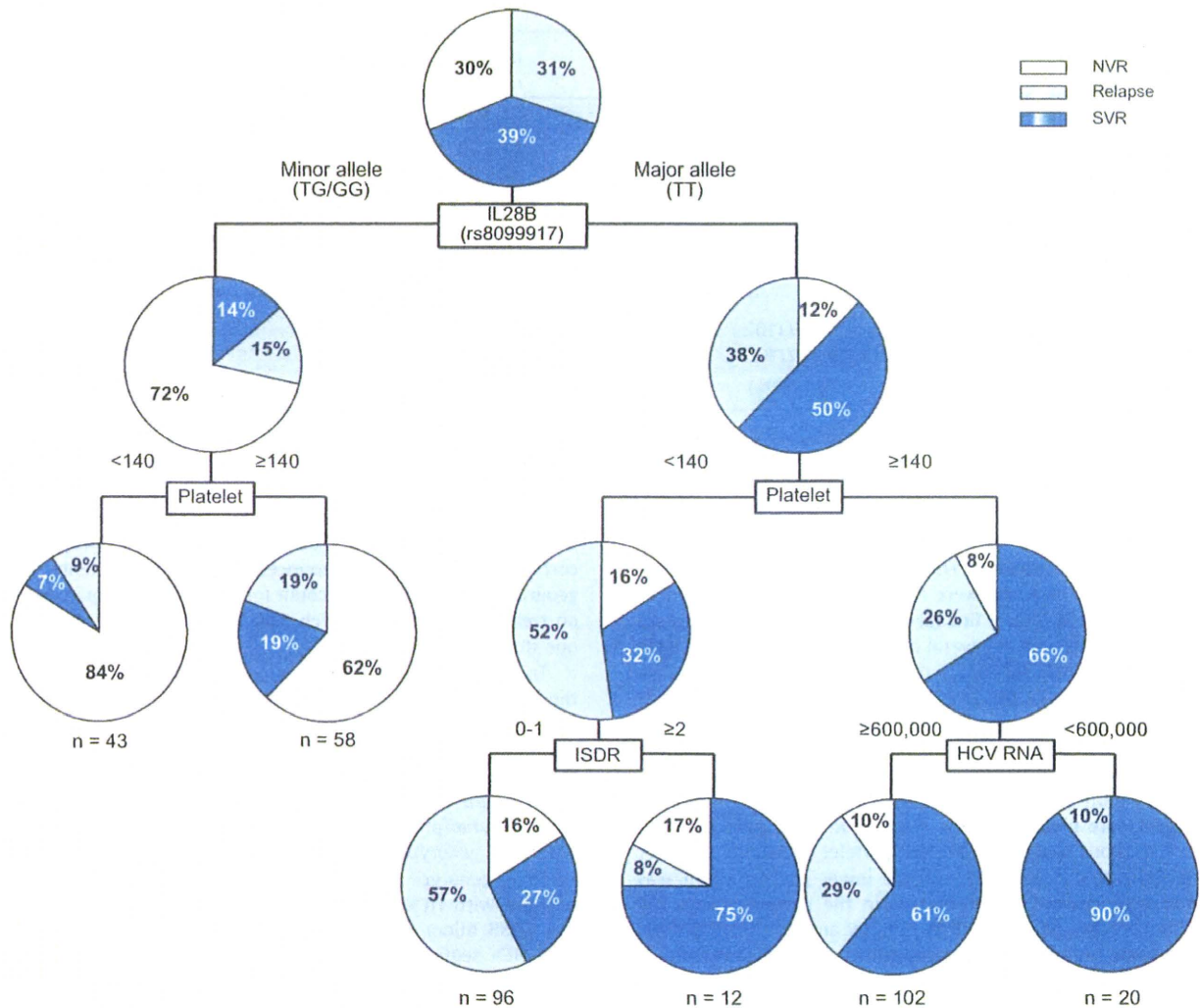


**Fig. 5. Decision tree for the prediction of response to therapy.** The boxes indicate the factors used for splitting. Pie charts indicate the rate of response for each group of patients after splitting. The rate of null virological response, relapse, and sustained virological response is shown. [This figure appears in colour on the web.]

group of patients. Using this model, we can rapidly develop an estimate of the response before treatment, by simply allocating patients to subgroups by following the flow-chart form, which may facilitate clinical decision making. This is in contrast to the calculating formula, which was constructed by the traditional logistic regression model. This was not widely used in clinical practice as it is abstruse and inconvenient. These results support the evidence based approach of selecting the optimum treatment strategy for individual patients, such as treating patients with a low probability of NVR with current PEG-IFN/RBV combination therapy or advising those with a high probability of NVR to wait for more effective future therapies. Patients with a high probability of relapse may be treated for a longer duration to avoid a relapse. Decisions may be based on the possibility of a response against a potential risk of adverse events and the cost of the therapy, or disease progression while waiting for future therapy.

We have previously reported the predictive model of early virological response to PEG-IFN and RBV in chronic hepatitis C

[26]. The top factor selected as significant was the grade of steatosis, followed by serum level of LDL cholesterol, age, GGT, and blood sugar. The mechanism of association between these factors and treatment response was not clear at that time. To our interest, a recent study by Li et al. [47] has shown that high serum level of LDL cholesterol was linked to the IL28B major allele (CC in rs12979860). High serum level of LDL cholesterol was associated with SVR but it was no longer significant when analyzed together with the IL28B genotype in multivariate analysis. Thus, the association between treatment response and LDL cholesterol levels may reflect the underlining link of LDL cholesterol levels to IL28B genotype. Steatosis is reported to be correlated with low lipid levels [48] which suggest that IL28B genotypes may be also associated with steatosis. In fact, there were significant correlations between the IL28B genotype and the presence of steatosis in the present study (Table 4). In addition, the serum level of GGT, another predictive factor in our previous study, was significantly associated with IL28B genotype in the present study

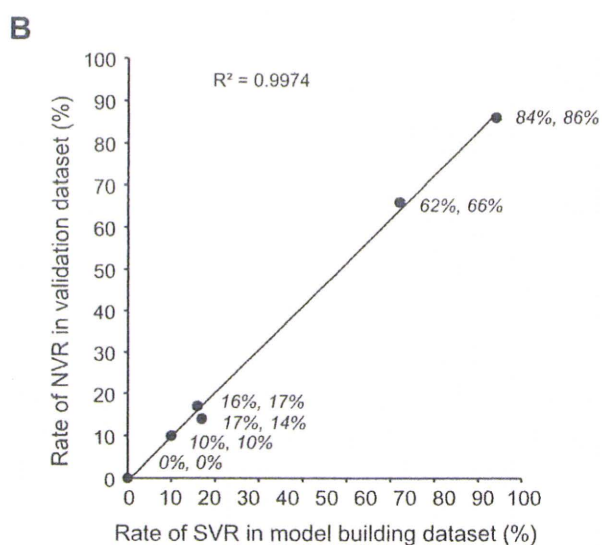
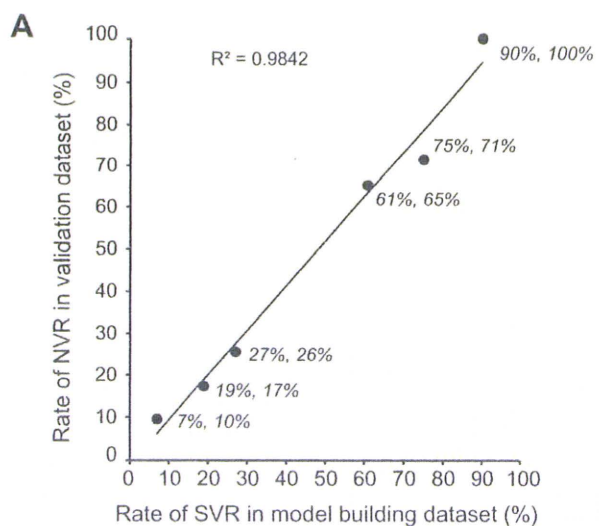


**Fig. 6. Validation of the CART analysis.** Each patient in the validation group was allocated to one of the six subgroups by following the flow-chart form of the decision tree. The rate of (A) sustained virological response (SVR) and (B) null virological response (NVR) in each subgroup was calculated and plotted. The X-axis represents the rate of SVR or NVR in the model building patients and the Y-axis represents those in the validation patients. The rate of SVR and NVR in each subgroup of patients is closely correlated to the model building and the validation patients (correlation coefficient:  $r^2 = 0.98-0.99$ ).

(Table 4). The serum level of GGT was significantly associated with NVR when examined independently but was no longer significant when analyzed together with the IL28B genotype. These observations indicate that some of the factors that we have previously identified may be associated with virological response to therapy through the underlining link to the IL28B genotype.

In conclusion, the present study highlighted the impact of the IL28B polymorphism and mutation in the ISDR on the pre-treatment prediction of response to PEG-IFN/RBV therapy. A decision model including these host and viral factors has the potential to

support selection of the optimum treatment strategy for individual patients, which may enable personalized treatment.

**Conflicts of interest**

The authors who have taken part in this study declare that they do not have anything to disclose regarding funding or conflict of interest with respect to this manuscript.

**Financial support**

This study was supported by a grant-in-aid from the Ministry of Health, Labor and Welfare, Japan, (H19-kannen-013), (H20-kannen-006).

**References**

- [1] Ray Kim W. Global epidemiology and burden of hepatitis C. *Microbes Infect* 2002;4 (12):1219-1225.
- [2] Fried MW, Shiffman ML, Reddy KR, Smith C, Marinos G, Goncalves Jr FL, et al. Peginterferon alfa-2a plus ribavirin for chronic hepatitis C virus infection. *N Engl J Med* 2002;347 (13):975-982.
- [3] Manns MP, McHutchison JG, Gordon SC, Rustgi VK, Shiffman M, Reindollar R, et al. Peginterferon alfa-2b plus ribavirin compared with interferon alfa-2b plus ribavirin for initial treatment of chronic hepatitis C: a randomised trial. *Lancet* 2001;358 (9286):958-965.
- [4] Akuta N, Suzuki F, Sezaki H, Suzuki Y, Hosaka T, Someya T, et al. Association of amino acid substitution pattern in core protein of hepatitis C virus genotype 1b high viral load and non-virological response to interferon-ribavirin combination therapy. *Intervirology* 2005;48 (6):372-380.
- [5] Davis GL, Wong JB, McHutchison JG, Manns MP, Harvey J, Albrecht J. Early virologic response to treatment with peginterferon alfa-2b plus ribavirin in patients with chronic hepatitis C. *Hepatology* 2003;38 (3):645-652.
- [6] Tanaka Y, Nishida N, Sugiyama M, Kurosaki M, Matsuura K, Sakamoto N, et al. Genome-wide association of IL28B with response to pegylated interferon-alpha and ribavirin therapy for chronic hepatitis C. *Nat Genet* 2009;41:1105-1109.
- [7] Suppiah V, Moldovan M, Ahlenstiel G, Berg T, Wilmann M, Abate ML, et al. IL28B is associated with response to chronic hepatitis C interferon-alpha and ribavirin therapy. *Nat Genet* 2009;41:1100-1104.
- [8] Ge D, Fellay J, Thompson AJ, Simon JS, Shianna KV, Urban TJ, et al. Genetic variation in IL28B predicts hepatitis C treatment-induced viral clearance. *Nature* 2009;461 (7262):399-401.
- [9] Rauch A, Kutalik Z, Descombes P, Cai T, Di Iulio J, Mueller T, et al. Genetic variation in IL28B is associated with chronic hepatitis C and treatment failure: a genome-wide association study. *Gastroenterology* 2010;138 (4):1338-1345.
- [10] Enomoto N, Sakuma I, Asahina Y, Kurosaki M, Murakami T, Yamamoto C, et al. Comparison of full-length sequences of interferon-sensitive and resistant hepatitis C virus 1b. Sensitivity to interferon is conferred by amino acid substitutions in the NS5A region. *J Clin Invest* 1995;96 (1):224-230.
- [11] Enomoto N, Sakuma I, Asahina Y, Kurosaki M, Murakami T, Yamamoto C, et al. Mutations in the nonstructural protein 5A gene and response to interferon in patients with chronic hepatitis C virus 1b infection. *N Engl J Med* 1996;334 (2):77-81.
- [12] Kurosaki M, Enomoto N, Murakami T, Sakuma I, Asahina Y, Yamamoto C, et al. Analysis of genotypes and amino acid residues 2209 to 2248 of the NS5A region of hepatitis C virus in relation to the response to interferon-beta therapy. *Hepatology* 1997;25 (3):750-753.
- [13] Shirakawa H, Matsumoto A, Joshita S, Komatsu M, Tanaka N, Umemura T, et al. Pretreatment prediction of virological response to peginterferon plus ribavirin therapy in chronic hepatitis C patients using viral and host factors. *Hepatology* 2008;48 (6):1753-1760.
- [14] Akuta N, Suzuki F, Kawamura Y, Yatsuji H, Sezaki H, Suzuki Y, et al. Predictive factors of early and sustained responses to peginterferon plus ribavirin combination therapy in Japanese patients infected with hepatitis C virus genotype 1b: amino acid substitutions in the core region and low-density lipoprotein cholesterol levels. *J Hepatol* 2007;46 (3):403-410.

Please cite this article in press as: Kurosaki M et al. Pre-treatment prediction of response to pegylated-interferon plus ribavirin for chronic hepatitis C using genetic polymorphism in IL28B and viral factors. *J Hepatol* (2010), doi:10.1016/j.jhep.2010.07.037



## Research Article

- [15] Okanoue T, Itoh Y, Hashimoto H, Yasui K, Minami M, Takehara T, et al. Predictive values of amino acid sequences of the core and NS5A regions in antiviral therapy for hepatitis C: a Japanese multi-center study. *J Gastroenterol* 2009;44 (9):952–963.
- [16] Segal MR, Bloch DA. A comparison of estimated proportional hazards models and regression trees. *Stat Med* 1989;8 (5):539–550.
- [17] LeBlanc M, Crowley J. A review of tree-based prognostic models. *Cancer Treat Res* 1995;75:113–124.
- [18] Garzotto M, Beer TM, Hudson RG, Peters L, Hsieh YC, Barrera E, et al. Improved detection of prostate cancer using classification and regression tree analysis. *J Clin Oncol* 2005;23 (19):4322–4329.
- [19] Averbook BJ, Fu P, Rao JS, Mansour EG. A long-term analysis of 1018 patients with melanoma by classic Cox regression and tree-structured survival analysis at a major referral center: implications on the future of cancer staging. *Surgery* 2002;132 (4):589–602.
- [20] Leiter U, Buettner PG, Eigentler TK, Garbe C. Prognostic factors of thin cutaneous melanoma: an analysis of the central malignant melanoma registry of the german dermatological society. *J Clin Oncol* 2004;22 (18):3660–3667.
- [21] Valera VA, Walter BA, Yokoyama N, Koyama Y, Iiai T, Okamoto H, et al. Prognostic groups in colorectal carcinoma patients based on tumor cell proliferation and classification and regression tree (CART) survival analysis. *Ann Surg Oncol* 2007;14 (1):34–40.
- [22] Zlobec I, Steele R, Nigam N, Compton CC. A predictive model of rectal tumor response to preoperative radiotherapy using classification and regression tree methods. *Clin Cancer Res* 2005;11 (15):5440–5443.
- [23] Thabane M, Simunovic M, Akhtar-Danesh N, Marshall JK. Development and validation of a risk score for post-infectious irritable bowel syndrome. *Am J Gastroenterol* 2009;104 (9):2267–2274.
- [24] Wu BU, Johannes RS, Sun X, Tabak Y, Conwell DL, Banks PA. The early prediction of mortality in acute pancreatitis: a large population-based study. *Gut* 2008;57 (12):1698–1703.
- [25] Fonarow GC, Adams Jr KF, Abraham WT, Yancy CW, Boscardin WJ. Risk stratification for in-hospital mortality in acutely decompensated heart failure: classification and regression tree analysis. *Jama* 2005;293 (5):572–580.
- [26] Kurosaki M, Matsunaga K, Hirayama I, Tanaka T, Sato M, Yasui Y, et al. A predictive model of response to peginterferon ribavirin in chronic hepatitis C using classification and regression tree analysis. *Hepato Res* 2010;40 (3):251–260.
- [27] Nishida N, Tanabe T, Takasu M, Suyama A, Tokunaga K. Further development of multiplex single nucleotide polymorphism typing method, the DigiTag2 assay. *Anal Biochem* 2007;364 (1):78–85.
- [28] Hezode C, Forestier N, Dusheiko G, Ferenci P, Pol S, Goeser T, et al. Telaprevir and peginterferon with or without ribavirin for chronic HCV infection. *N Engl J Med* 2009;360 (18):1839–1850.
- [29] McHutchison JG, Everson GT, Gordon SC, Jacobson IM, Sulkowski M, Kauffman R, et al. Telaprevir with peginterferon and ribavirin for chronic HCV genotype 1 infection. *N Engl J Med* 2009;360 (18):1827–1838.
- [30] Rossignol JF, Elfert A, El-Gohary Y, Keeffe EB. Improved virologic response in chronic hepatitis C genotype 4 treated with nitazoxanide, peginterferon, and ribavirin. *Gastroenterology* 2009;136 (3):856–862.
- [31] Marcello T, Grakoui A, Barba-Spaeth G, Machlin ES, Kotelko SV, MacDonald MR, et al. Interferons alpha and lambda inhibit hepatitis C virus replication with distinct signal transduction and gene regulation kinetics. *Gastroenterology* 2006;131 (6):1887–1898.
- [32] Robek MD, Boyd BS, Chisari FV. Lambda interferon inhibits hepatitis B and C virus replication. *J Virol* 2005;79 (6):3851–3854.
- [33] McCarthy JJ, Li JH, Thompson A, Suchindran S, Lao XQ, Patel K, et al. Replicated association between an IL28B Gene Variant and a Sustained Response to Pegylated Interferon and Ribavirin. *Gastroenterology* 2010;138:2307–2314.
- [34] Tanaka Y, Nishida N, Sugiyama M, Tokunaga K, Mizokami M.  $\Lambda$ -interferons and the single nucleotide polymorphisms: a milestone to tailor-made therapy for chronic hepatitis C. *Hepato Res* 2010;40:449–460.
- [35] Backus LI, Boothroyd DB, Phillips BR, Mole LA. Predictors of response of US veterans to treatment for the hepatitis C virus. *Hepatology* 2007;46 (1):37–47.
- [36] Mori N, Imamura M, Kawakami Y, Saneto H, Kawaoka T, Takaki S, et al. Randomized trial of high-dose interferon-alpha-2b combined with ribavirin in patients with chronic hepatitis C: correlation between amino acid substitutions in the core/NS5A region and virological response to interferon therapy. *J Med Virol* 2009;81 (4):640–649.
- [37] Hung CH, Lee CM, Lu SN, Lee JF, Wang JH, Tung HD, et al. Mutations in the NS5A and E2-PePHD region of hepatitis C virus type 1b and correlation with the response to combination therapy with interferon and ribavirin. *J Viral Hepat* 2003;10 (2):87–94.
- [38] Yen YH, Hung CH, Hu TH, Chen CH, Wu CM, Wang JH, et al. Mutations in the interferon sensitivity-determining region (nonstructural 5A amino acid 2209–2248) in patients with hepatitis C-1b infection and correlating response to combined therapy of pegylated interferon and ribavirin. *Aliment Pharmacol Ther* 2008;27 (1):72–79.
- [39] Zeuzem S, Lee JH, Roth WK. Mutations in the nonstructural 5A gene of European hepatitis C virus isolates and response to interferon alfa. *Hepatology* 1997;25 (3):740–744.
- [40] Squadrito G, Leone F, Sartori M, Nalpas B, Berthelot P, Raimondo G, et al. Mutations in the nonstructural 5A region of hepatitis C virus and response of chronic hepatitis C to interferon alfa. *Gastroenterology* 1997;113 (2):567–572.
- [41] Sarrazin C, Berg T, Lee JH, Teuber G, Dietrich CF, Roth WK, et al. Improved correlation between multiple mutations within the NS5A region and virological response in European patients chronically infected with hepatitis C virus type 1b undergoing combination therapy. *J Hepato Res* 1999;30 (6):1004–1013.
- [42] Murphy MD, Rosen HR, Marousek GI, Chou S. Analysis of sequence configurations of the ISDR, PKR-binding domain, and V3 region as predictors of response to induction interferon-alpha and ribavirin therapy in chronic hepatitis C infection. *Dig Dis Sci* 2002;47 (6):1195–1205.
- [43] Pascu M, Martus P, Hohne M, Wiedenmann B, Hopf U, Schreiber E, et al. Sustained virological response in hepatitis C virus type 1b infected patients is predicted by the number of mutations within the NS5A-ISDR: a meta-analysis focused on geographical differences. *Gut* 2004;53 (9):1345–1351.
- [44] Thomas DL, Thio CL, Martin MP, Qi Y, Ge D, O'Huigin C, et al. Genetic variation in IL28B and spontaneous clearance of hepatitis C virus. *Nature* 2009;461 (7265):798–801.
- [45] Kurosaki M, Enomoto N, Marumo F, Sato C. Evolution and selection of hepatitis C virus variants in patients with chronic hepatitis C. *Virology* 1994;205 (1):161–169.
- [46] Enomoto N, Kurosaki M, Tanaka Y, Marumo F, Sato C. Fluctuation of hepatitis C virus quasispecies in persistent infection and interferon treatment revealed by single-strand conformation polymorphism analysis. *J Gen Virol* 1994;75 (Pt 6):1361–1369.
- [47] Li JH, Lao XQ, Tillmann HL, Rowell J, Patel K, Thompson A, et al. Interferon-lambda genotype and low serum low-density lipoprotein cholesterol levels in patients with chronic hepatitis C infection. *Hepatology* 1904;51 (6):1904–1911.
- [48] Serfaty L, Andreani T, Giral P, Carbonell N, Chazouilleres O, Poupon R. Hepatitis C virus induced hypobetalipoproteinemia: a possible mechanism for steatosis in chronic hepatitis C. *J Hepato Res* 2001;34 (3):428–434.

# Involvement of PA28 $\gamma$ in the Propagation of Hepatitis C Virus

Kohji Moriishi,<sup>1</sup> Ikuro Shoji,<sup>2</sup> Yoshio Mori,<sup>1</sup> Ryosuke Suzuki,<sup>3</sup> Tetsuro Suzuki,<sup>3</sup> Chikako Kataoka,<sup>1</sup> and Yoshiharu Matsuura<sup>1</sup>

We have reported previously that the proteasome activator PA28 $\gamma$  participates not only in degradation of hepatitis C virus (HCV) core protein in the nucleus but also in the pathogenesis in transgenic mice expressing HCV core protein. However, the biological significance of PA28 $\gamma$  in the propagation of HCV has not been clarified. PA28 $\gamma$  is an activator of proteasome responsible for ubiquitin-independent degradation of substrates in the nucleus. In the present study, knockdown of PA28 $\gamma$  in cells preinfection or postinfection with the JFH-1 strain of HCV impaired viral particle production but exhibited no effect on viral RNA replication. The particle production of HCV in PA28 $\gamma$  knockdown cells was restored by the expression of an small interfering RNA (siRNA)-resistant PA28 $\gamma$ . Although viral proteins were detected in the cytoplasm of cells infected with HCV, suppression of PA28 $\gamma$  expression induced accumulation of HCV core protein in the nucleus. HCV core protein was also degraded in the cytoplasm after ubiquitination by an E3 ubiquitin ligase, E6AP. Knockdown of PA28 $\gamma$  enhanced ubiquitination of core protein and impaired virus production, whereas that of E6AP reduced ubiquitination of core protein and enhanced virus production. Furthermore, virus production in the PA28 $\gamma$  knockdown cells was restored through knockdown of E6AP or expression of the siRNA-resistant wild-type but not mutant PA28 $\gamma$  incapable of activating proteasome activity. **Conclusion:** Our results suggest that PA28 $\gamma$  participates not only in the pathogenesis but also in the propagation of HCV by regulating the degradation of the core protein in both a ubiquitin-dependent and ubiquitin-independent manner. (HEPATOLOGY 2010;52:411-420)

Over 170 million individuals worldwide are infected with hepatitis C virus (HCV), which is a major etiological agent of liver diseases, including hepatic steatosis, cirrhosis, and hepatocellular carcinoma (HCC).<sup>1</sup> HCV is classified into the genus

Hepacivirus of the *Flaviviridae* family and has a positive, single-strand RNA genome that encodes a single polyprotein consisting of about 3,000 amino acids.<sup>2</sup> The N-terminal one-third of the polyprotein is occupied by the structural proteins, and the remaining portion consists of nonstructural proteins involved in viral replication and assembly. Host and viral proteases cleave the appropriate sites of the polyprotein, resulting in generation of at least 10 viral proteins. The capsid (core), E1 and E2 proteins, and p7 are cleaved off by signal peptidase from the polyprotein. Furthermore, the C-terminal signal sequence of the core protein is processed by signal peptide peptidase.<sup>3</sup> Our recent data indicate that signal peptide peptidase cleaves the polyprotein between Phe<sup>177</sup> and Leu<sup>178</sup> in the signal sequence, and this processing is required for HCV propagation.<sup>4</sup> The mature core proteins make nucleocapsid with viral RNA, and HCV particles bud into the lumen of the endoplasmic reticulum bearing E1 and E2 glycoproteins on the host lipid components, and are released from the host cells.

Several reports suggest that HCV core protein plays an important role in the development of various outcomes of liver failure, including steatosis and HCC.<sup>5,6</sup>

*Abbreviations:* HA, hemagglutinin; HCC, hepatocellular carcinoma; HCV, hepatitis C virus; JEV, Japanese encephalitis virus; moi, multiplicity of infection; shRNA, short hairpin RNA; siRNA, small interfering RNA.

From the <sup>1</sup>Department of Molecular Virology, Research Institute for Microbial Diseases, Osaka University, Osaka, Japan; the <sup>2</sup>Division of Microbiology, Kobe University Graduate School of Medicine, Hyogo, Japan; and the <sup>3</sup>Department of Virology II, National Institute of Infectious Diseases, Tokyo, Japan.

Received February 3, 2010; accepted March 13, 2010.

Supported in part by grants-in-aid from the Ministry of Health, Labor, and Welfare; the Ministry of Education, Culture, Sports, Science, and Technology; the Osaka University Global Center of Excellence Program; and the Foundation for Biomedical Research and Innovation.

Potential conflict of interest: Nothing to report.

Address reprint requests to: Yoshiharu Matsuura, D.V.M., Ph.D., Department of Molecular Virology, Research Institute for Microbial Diseases, Osaka University, 3-1 Yamada-oka, Suita, Osaka 565-0871, Japan. E-mail: matsuura@biken.osaka-u.ac.jp; fax: (81)-6-6879-8269.

Copyright © 2010 by the American Association for the Study of Liver Diseases.

Published online in Wiley InterScience (www.interscience.wiley.com).

DOI 10.1002/hep.23680

Additional Supporting Information may be found in the online version of this article.

We have reported previously that HCV core protein specifically interacts with a proteasome activator PA28 $\gamma$ /REG $\gamma$  in the nucleus and is digested by a PA28 $\gamma$ -dependent proteasome activity.<sup>7</sup> *In vivo* experiments in a mouse model suggest that PA28 $\gamma$  plays a critical role in the pathogenesis induced by HCV core protein.<sup>8,9</sup> PA28 $\gamma$  forms a homoheptamer in the nucleus and enhances the proteasome-mediated cleavage after basic amino acid residues, whereas PA28 $\alpha$  and PA28 $\beta$  exhibit 41% and 34% homology to PA28 $\gamma$ , respectively, and form a heteroheptamer in the cytoplasm to activate cleavage after hydrophobic, acidic, or basic amino acid residues.<sup>10</sup> Recently, several groups reported that PA28 $\gamma$  interacts with steroid receptor coactivator-3 and cell cycle suppressors such as p21<sup>WAF1/CIP1</sup>, p16<sup>INK4A</sup>, and p19<sup>ARF</sup>, and enhances the degradation of these proteins in a ubiquitin- and adenosine triphosphate-independent manner.<sup>11-13</sup> Furthermore, other mechanisms of ubiquitin-independent degradation have been considered for cell cycle regulation, summarized in the review of Jariel-Encontre et al.<sup>14</sup> However, the precise physiological functions of PA28 $\gamma$  are largely unknown *in vivo*, because PA28 $\gamma$ -knockout mice exhibit only mild growth retardation and live approximately as long as their control littermates.<sup>15,16</sup>

HCV core protein is degraded in a PA28 $\gamma$ -dependent and ubiquitin-independent manner in the nucleus,<sup>7,17</sup> while E6AP is also involved in the degradation of the core protein in a ubiquitin-dependent manner.<sup>17,18</sup> E6AP is a member of E3 ligases, which catalyze ubiquitin ligation of host and foreign proteins. Knockdown of E6AP suppressed degradation of HCV core protein and enhanced the release of infectious particles, suggesting that E6AP negatively regulates HCV propagation.<sup>18</sup> However, the role of PA28 $\gamma$  in the propagation of HCV has not yet been characterized. In this study, we examined the biological significance of PA28 $\gamma$  in the propagation of HCV.

## Materials and Methods

**Transfection, Immunoblotting, and RNA Interference.** Plasmid DNA was transfected into Huh7OK1 cells by way of liposome-mediated transfection using Lipofectamine LTX with Plus reagent (Invitrogen, Carlsbad, CA). Expression of HCV core protein was determined by way of enzyme-linked immunosorbent assay as described.<sup>19</sup> Immunoblotting was performed as described.<sup>8</sup> The small interfering RNAs (siRNAs) targeted to the PA28 $\gamma$  gene were purchased from

Ambion (Austin, TX) and were introduced into the cell lines using Lipofectamine RNAiMax (Invitrogen). siRNAs with the Ambion siRNA ID numbers 138669 and 138670 were designated as siPA28 $\gamma$ 1 and siPA28 $\gamma$ 2, respectively. Antibodies and plasmids are described in the Supporting Information.

**Cell Lines and Virus Infection.** All cell lines were cultured at 37°C under the conditions of humidified atmosphere and 5% CO<sub>2</sub>. The human hepatoma cell line Huh7OK1 and derivative cell lines were maintained in Dulbecco's modified Eagle's medium (Sigma, St. Louis, MO) supplemented with nonessential amino acids, sodium pyruvate, and 10% fetal bovine serum. The Huh7-derived cell line harboring a subgenomic or a full-length HCV replicon RNA<sup>20</sup> was maintained in Dulbecco's modified Eagle's medium containing 10% fetal bovine serum, nonessential amino acids, sodium pyruvate, and 1 mg/mL G418 (Nakarai Tesque, Kyoto, Japan). Huh7OK1 cells were transfected with pSilencer-shPA28 $\gamma$ 4 or a control plasmid, pSilencer 2.1 U6 hygro negative control (Ambion), and drug-resistant clones were selected by treatment with hygromycin (Wako, Tokyo, Japan) at a final concentration of 100  $\mu$ g/mL. Huh7OK1 cells transfected with the control plasmid were selected with puromycin and designated as shCntrl, whereas those transfected with pSilencer-shPA28 $\gamma$ 4 were established by limited dilution,<sup>8</sup> and two of the resulting cell lines were designated as KD5 and KD7. Plasmids encoding wild-type or mutant PA28 $\gamma$  complementary DNAs resistant to siRNA against PA28 $\gamma$  were prepared by using the silent mutations as reported.<sup>8</sup> These plasmids were transfected into Huh7OK1 cells and cultivated in medium containing 0.1  $\mu$ g/mL of puromycin for 2 days. The surviving cells were used for virus infection. The shCtrl and KD5 cells were transformed with pSilencer shE6AP or pSilencer 3.1 H1 puro negative control (Ambion) and treated with 0.1  $\mu$ g/mL of puromycin for 2 days. The surviving cells were infected with JFH-1 virus at a multiplicity of infection (moi) of 0.05. The viral RNA derived from the plasmid pJFH1 was transcribed and introduced into Huh7OK1 cells according to the method of Wakita et al.<sup>21</sup> The infectivity of JFH1 strain was determined using a focus-forming assay<sup>21</sup> and is expressed in focus-forming units. The Huh7 cell line harboring subgenomic replicon RNA of the Con1 or JFH1 strain was prepared according to the method of Pietschmann et al.<sup>22</sup> The infectivity of the Japanese encephalitis virus (JEV) was determined by an immunostaining focus assay as described<sup>23</sup> and is expressed in focus-forming units. Colony formation and replication assays, quantitative

reverse-transcription polymerase chain reaction, and estimation of cell growth was performed as described in the Supporting Information.

**Immunofluorescent Staining.** Huh7OK1-derived cells were seeded at  $0.5 \times 10^4$  cells/well in an eight-well chamber slide, infected with JFH-1 virus at an moi of 0.3 after incubation at 37°C for 24 hours, stained with Bodipy 558/568 C<sub>12</sub> according to the method of Targett-Adams et al.<sup>24</sup> at 4 days postinfection, and then fixed at 4°C for 30 minutes with 4% paraformaldehyde in phosphate-buffered saline. After treatment of cells with 1 μg/mL of RNase A, nuclei were stained with 50 μM Hechst 33258. The fixed cells were permeabilized with 20 mM Tris-HCl containing 1% Nonidet P-40 and 135 mM NaCl at room temperature for 5 minutes, reacted with rabbit anti-core or anti-NS5A antibody followed by Alexa Fluor 488-goat antibody to rabbit immunoglobulin G, washed three times with phosphate-buffered saline, and observed with a FluoView FV1000 laser scanning confocal microscope (Olympus, Tokyo, Japan). The percentage of the area occupied by the core protein in nucleus and cytoplasm was calculated using Image-Pro software (Media Cybernetics). The percentage of the nuclear core protein to the total core protein was examined randomly in 10 fields of every three wells. The percentage of the nuclear NS5A to total NS5A was estimated by the same method as the ratio of the core protein.

## Results

**Transient Knockdown of PA28 $\gamma$  Prior to or After Infection With HCV Reduces Particle Production.** We reported previously that Huh7OK1 cells are as permissive to JFH-1 virus infection as Huh7.5.1 cells.<sup>25</sup> The Huh7OK1 cell line retained the ability to produce type I IFNs through the RIG-I-dependent signaling pathway upon infection with RNA viruses and exhibited a cell surface expression level of human CD81 comparable to that of the parental cell line. However, the mechanism through which the Huh7OK1 cell line exhibits highly permissive to JFH-1 virus infection has not been clarified yet. Two siRNAs were used to knock down PA28 $\gamma$ , but only one, siPA28 $\gamma$ 1, was used because the other had off-target effects (Supporting Fig. 1). To examine the effect of PA28 $\gamma$  on the propagation of HCV, siPA28 $\gamma$ 1 was introduced into Huh7OK1 cells 24 hours before infection. The levels of viral RNA, core protein, and infectious viral titer were determined at 48 and 96 hours postinfection. Viral RNA in the culture supernatant and cells was clearly reduced by the knockdown of

PA28 $\gamma$  at 48 and 96 hours postinfection, respectively (Fig. 1A), whereas a significant reduction of core protein expression was detected at 96 hours but not at 48

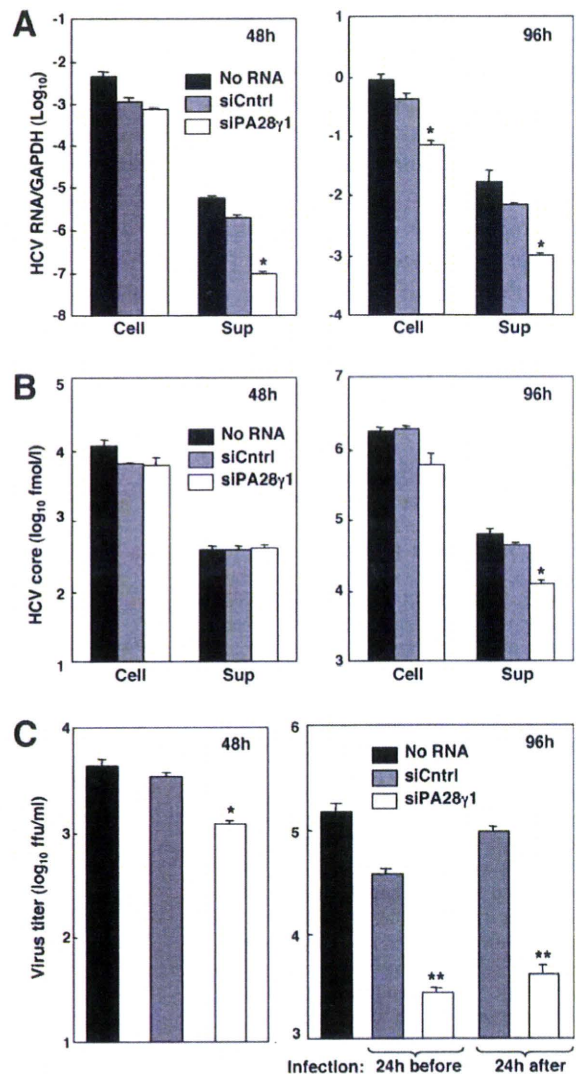
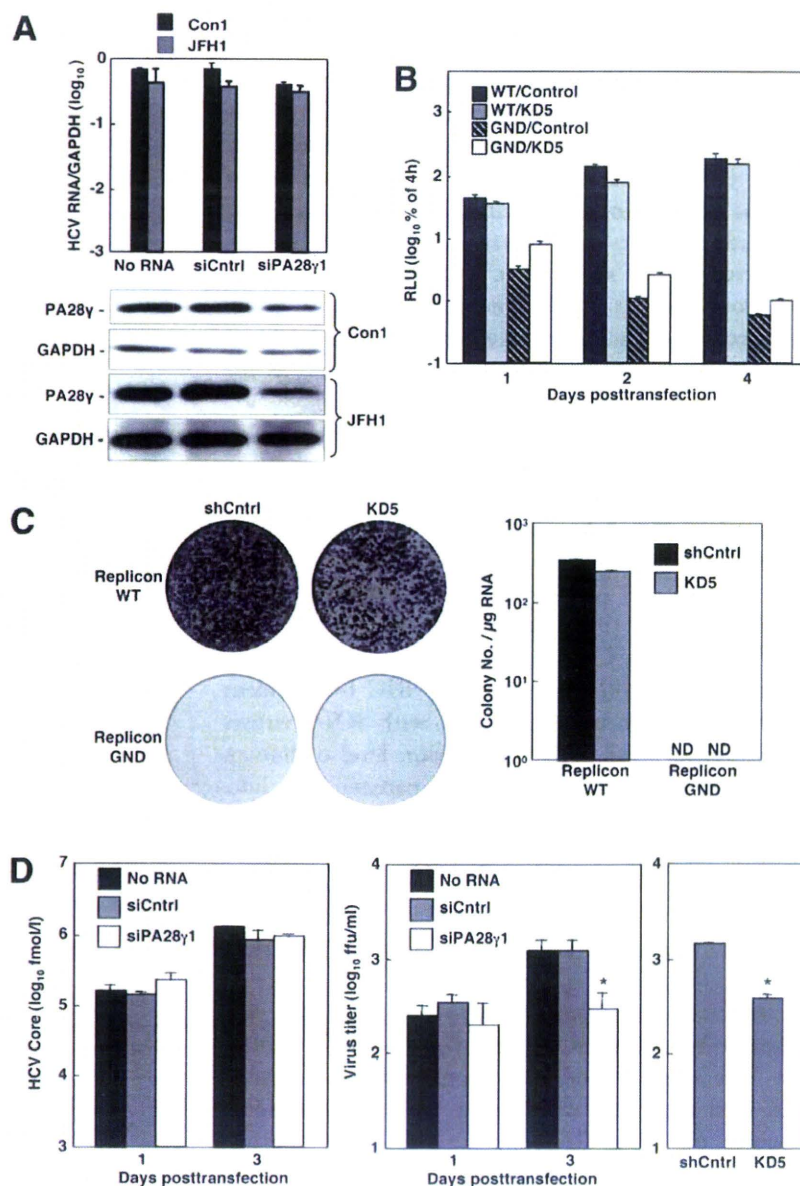


Fig. 1. Transient knockdown of PA28 $\gamma$  before or after infection with HCV reduces particle production. (A) Huh7OK1 cells transfected with a control siRNA (siCtrl) or PA28 $\gamma$  siRNA1 were infected with JFH-1 virus at 24 hours posttransfection and then harvested at 48 hours (left panel) and 96 hours postinfection (right panel). The quantity of HCV RNA in cells and supernatants was determined by way of quantitative reverse-transcription polymerase chain reaction. (B) The expression of HCV core protein in cells and supernatants at 48 hours (left panel) and 96 hours (right panel) postinfection was determined by ELISA. (C) Huh7OK1 cells that were transfected with siCtrl or PA28 $\gamma$  siRNA1 were infected with JFH-1 virus at 24 hours posttransfection. The infectivity of the virus in the culture supernatant was determined by a focus-forming assay at 48 hours postinfection (left panel). Those transfected with the siRNAs at 24 hours before and after infection with JFH-1 virus were determined similarly at 96 hours postinfection (right panel). \* $P < 0.05$ , \*\* $P < 0.01$  versus control siRNA-transfected cells. Data are representative of three independent experiments.

knockdown cell line KD5 and the control cell line transfected with the subgenomic replicon RNA (WT) were gradually increased until 4 days posttransfection, whereas luciferase activities in the same two cell lines transfected with the polymerase-dead replicon RNA (GND) were decreased in a time-dependent manner (Fig. 3B). Next, to explore the effect of PA28 $\gamma$  knockdown on the viral replication over a longer period, replicon RNA encoding the neomycin-resistance gene was transfected into the cell lines for a colony formation assay. The numbers of colonies in the KD5 cell line after 4 weeks of selection with G418 were similar to those in the control cell line (Fig. 3C). To further clarify the roles of PA28 $\gamma$  on the postreplication steps,

*in vitro* transcribed full-length viral RNA was transfected into Huh7OK1 cells, and siPA28 $\gamma$ 1 was then introduced into the cells at 24 hours posttransfection of viral RNA. Intracellular core protein was increased in a time-dependent manner, but no significant difference was observed between cells transfected with control siRNA and those transfected with siPA28 $\gamma$ 1 (Fig. 3D, left panel). However, infectious virus titers in the supernatant were significantly decreased by the transient and stable knockdown of PA28 $\gamma$  compared with control cells (Fig. 3D, middle and right panels). Furthermore, PA28 $\gamma$  did not contribute to the virus production of JEV (Fig. 2F), suggesting that the general sorting pathway of the flavivirus is functional under

Fig. 3. Effect of PA28 $\gamma$  knockdown on HCV RNA replication. (A) The siCntrl or siPA28 $\gamma$ 1 (10 nM) was transfected into the subgenomic HCV replicon cells derived from Con1 and JFH-1 strains. The transfected cells were harvested at 72 hours posttransfection. The replicon RNA was determined by quantitative reverse-transcription polymerase chain reaction at 72 hours posttransfection (upper). PA28 $\gamma$  or glyceraldehyde 3-phosphate dehydrogenase was detected by way of immunoblotting. Cell lysates were subjected to western blotting using antibodies to PA28 $\gamma$  and glyceraldehyde 3-phosphate dehydrogenase (lower). (B) The HCV replicon RNA encoding luciferase gene (WT) or the HCV replicon RNA that has a replication-deficient mutation (GND) was transfected into the shCntrl (Control) and KD5 cell lines. Relative luciferase activity was determined using the activity at 4 hours post-electroporation as a transfection efficiency. (C) Colony formation assay. Replicon RNA encoding the neomycin-resistance gene was transfected into the shCntrl and KD5 cell lines, and the remaining colonies were fixed with 4% paraformaldehyde at 4 weeks posttransfection and then stained with crystal violet. The number of colonies was counted (right). (D) Huh7OK1 cells transfected with 10  $\mu$ g of *in vitro*-transcribed full-length JFH-1 viral RNA were further transfected with siCntrl or siPA28 $\gamma$ 1 at 24 hours posttransfection of viral RNA. The level of HCV core protein in the cells was determined by way of ELISA at 1 and 3 days posttransfection (left). Infectious virus titers in the culture supernatants at 1 and 3 days posttransfection were determined by way of focus-forming assay (middle). Infectious viral titers in the shCntrl or KD5 cells transfected with 10  $\mu$ g of the infectious viral RNA were determined at 5 days posttransfection (right). \* $P$  < 0.05, \*\* $P$  < 0.01 versus the control cells or cells transfected with siCntrl. Data are representative of three independent experiments.



hours postinfection (Fig. 1B). Infectious viral titer in the culture supernatant was significantly reduced at 48 and 96 hours postinfection by the PA28 $\gamma$  knockdown (Fig. 1C), consistent with the suppression of the viral RNA in the supernatant. Furthermore, a comparable suppression of the production of infectious particles in the supernatant was also achieved by introducing siPA28 $\gamma$ 1 into cells even at 24 hours postinfection (Fig. 1C, right panel). These results suggest that PA28 $\gamma$  participates in the regulation of HCV propagation in postentry steps.

**Stable Knockdown of PA28 $\gamma$  Impairs Viral Propagation.** To establish the PA28 $\gamma$  knockdown cell lines, Huh7OK1 cells were transfected with a plasmid encoding a short hairpin RNA (shRNA) targeted to PA28 $\gamma$  and selected with hygromycin, resulting in two clones—KD5 and KD7—that exhibited a clear reduction of PA28 $\gamma$  expression (Fig. 2A). Although the suppression of PA28 $\gamma$  expression in KD7 cells was slightly more efficient than that in KD5 cells, the growth of KD7 cells was impaired (Fig. 2B). Viral production in the culture supernatants in cells infected with the JFH-1 virus was significantly impaired in PA28 $\gamma$  knockdown KD5 cells compared with control cells (Fig. 2C). The viral RNA and core protein in the supernatant were also reduced in KD5 cells (Fig. 2D). Expression of siRNA-resistant PA28 $\gamma$  in PA28 $\gamma$  knockdown KD5 and KD7 cells recovered virus production in the supernatant to a level similar to that in the control cells transfected with an empty vector, and overexpression of siRNA-resistant PA28 $\gamma$  in control cells slightly enhanced virus production (Fig. 2E). Our previous data suggest that capsid protein of JEV does not bind to PA28 $\gamma$ .<sup>7</sup> To examine whether PA28 $\gamma$  regulates JEV propagation, KD5 and shCntrl cells were infected with JEV at an moi of 0.5. The infectivity of JEV in KD5 cells was similar to that in shCntrl cells (Fig. 2F), suggesting that PA28 $\gamma$  does not participate in the virus production pathway of JEV. These results further support the notion that PA28 $\gamma$  participates in HCV propagation.

**Knockdown of PA28 $\gamma$  Exhibits No Effect on Viral RNA Replication.** Although knockdown of PA28 $\gamma$  resulted in the suppression of viral particle and RNA production in the culture supernatant at 48 hours postinfection with JFH-1 virus, viral RNA in the cells was not reduced (Fig. 1), suggesting that PA28 $\gamma$  does not participate in viral replication. To gain more insight on this point, we examined the effect of PA28 $\gamma$  knockdown on RNA replication in replicon cells. Transient knockdown of PA28 $\gamma$  through introduction of siPA28 $\gamma$  into the subgenomic HCV replicon cells

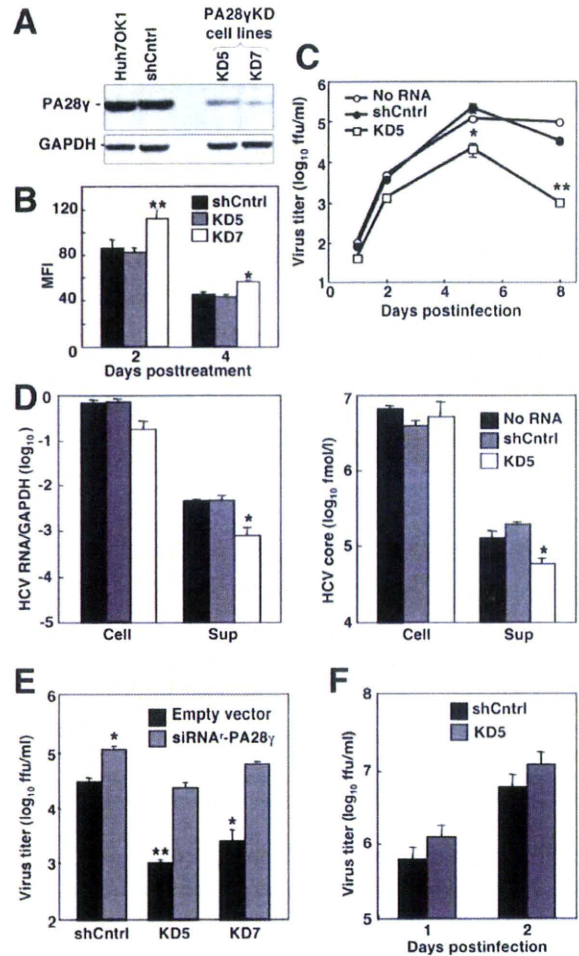


Fig. 2. Establishment of PA28 $\gamma$  knockdown cell lines and propagation of HCV. (A) Huh7OK1 cells were transfected with pSilencer shPA28 $\gamma$  or control plasmid and selected by hygromycin at 48 hours posttransfection. Two PA28 $\gamma$  knockdown cell lines (KD5 and KD7) and one control cell line (shCntrl) were established, and PA28 $\gamma$  knockdown was confirmed by way of immunoblotting. (B) Growth of the cell lines was determined by staining with carboxyfluorescein succinimidyl ester. (C,D) KD5 and shCntrl cell lines were infected with the JFH-1 virus at an moi of 0.05. The infectious virus titers in the culture supernatants (C) were determined by way of focus-forming assay. The virus RNA (D, left panel) and the core protein (D, right panel) in both cell and the supernatant were determined at 5 days postinfection by way of ELISA and quantitative reverse-transcription polymerase chain reaction, respectively. (E) The plasmid encoding an siRNA-resistant PA28 $\gamma$  or empty vector was transfected into the cell lines, seeded at  $5 \times 10^4$  cells into a six-well plate after cultivation in the presence of puromycin for 2 days, and infected with JFH-1 virus at an moi of 0.05. The viral titers were determined at 5 days postinfection. \* $P < 0.05$ , \*\* $P < 0.01$  versus shCntrl cells transfected with an empty vector. (F) KD5 and shCntrl cell lines were infected with the JEV virus at an moi of 0.5. The infectivity of JEV in the supernatant was determined at 1 and 2 days postinfection. Data are representative of three independent experiments.

derived from the Con1 or JFH-1 strain induced no significant reduction of HCV RNA (Fig. 3A). Furthermore, luciferase activities in the stable PA28 $\gamma$

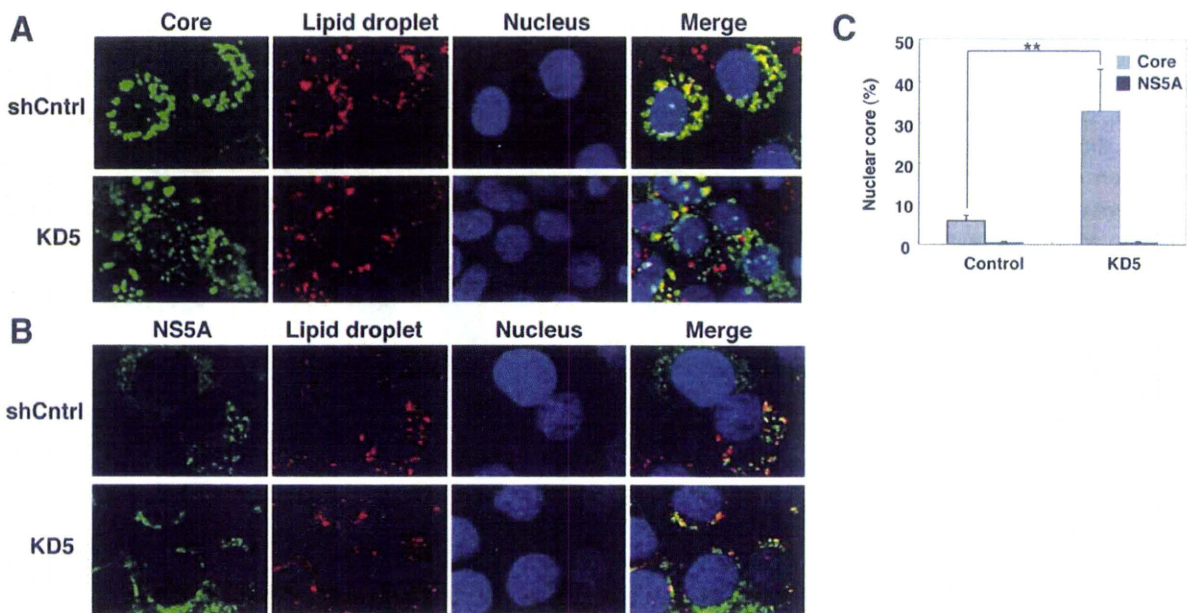


Fig. 4. Effect of PA28 $\gamma$  knockdown on the localization of HCV core protein and lipid droplets. The shCntrl and KD5 cell lines infected with JFH-1 virus were fixed with methanol or paraformaldehyde for 5 minutes at 4 days postinfection. HCV core (A) and NS5A (B) proteins were stained with rabbit antibodies raised against the proteins and Alexa Fluor 488-conjugated goat anti-rabbit immunoglobulin G antibody. Lipid droplets were stained with Bodipy 558/568 C12. Nuclei were stained with 50  $\mu$ M Hoechst 33258 after treatment with 1  $\mu$ g/mL of RNase A. Data are representative of three independent experiments. (C) The percentage of the area occupied by the core protein in nucleus and cytoplasm was calculated using the method described in Materials and Methods. The percentage of the nuclear NS5A to total NS5A was estimated by the same way as the ratio of the core protein. \*\* $P < 0.01$  versus control siRNA-transfected cells.

the PA28 $\gamma$  knockdown condition. These results suggest that PA28 $\gamma$  specifically regulates the postreplication steps in the life cycle of HCV.

**Core Protein Is Partially Accumulated in the Nucleus of PA28 $\gamma$  Knockdown Cells.** We reported previously that some fraction of HCV core protein migrates into the nucleus and is then degraded by a PA28 $\gamma$ -dependent proteasome pathway.<sup>7</sup> Furthermore, we have demonstrated that HCV core protein is clearly accumulated in the nucleus of the liver cells of PA28 $\gamma$ -knockout mice.<sup>8</sup> However, the role of PA28 $\gamma$  on the intracellular localization of HCV core protein in the infected HCV cells has not been characterized. HCV core protein was chiefly detected in cytoplasm of the control cell line infected with the JFH-1 virus, where it appeared around lipid droplets after staining with Bodipy 558/568 C12 (Fig. 4A, upper panels). In contrast, the core protein was detected not only in the cytoplasm around the surface of lipid droplets, but also in the nucleus in the KD5 cell line (Fig. 4A, lower panels). The NS5A protein was detected in the cytoplasm but not in the nucleus in both the shCntrl and KD5 cell lines (Fig. 4B). The percentage occupied by nuclear core protein to total core protein was increased by about six time levels in the KD5, while the ratio of nuclear NS5A to total NS5A exhibited no

difference (Fig. 4C). These results suggest that PA28 $\gamma$  participates in the degradation of HCV core protein in the nucleus.

**PA28 $\gamma$  Positively Regulates HCV Propagation by Inhibiting Ubiquitin-Dependent Degradation of Core Protein in Cytoplasm.** We reported previously that HCV core protein is degraded by at least two distinct pathways: a ubiquitin-dependent proteasome pathway and a ubiquitin-independent proteasome pathway.<sup>17</sup> The ubiquitin E3 ligase, E6AP, can catalyze ubiquitin ligation of the core protein for ubiquitin-dependent degradation in the cytoplasm,<sup>18</sup> whereas PA28 $\gamma$  participates in the degradation of the core protein through a ubiquitin-independent pathway in the nucleus.<sup>17</sup> We have also demonstrated that PA28 $\gamma$  knockdown leads to enhanced ubiquitination of HCV core protein.<sup>8</sup> However, the interplay between these two pathways in cells infected with HCV has not been determined. To address this point, we examined the effects of knockdown of E6AP or PA28 $\gamma$  on the virus propagation and the ubiquitination of the core protein. JFH-1 virus was inoculated into E6AP- and/or PA28 $\gamma$  knockdown cell lines (Fig. 5A). Transfection of the plasmid encoding shRNA to E6AP into the control cells (shCntrl) increased virus production (Fig. 5A [C-E]) in comparison with that of the

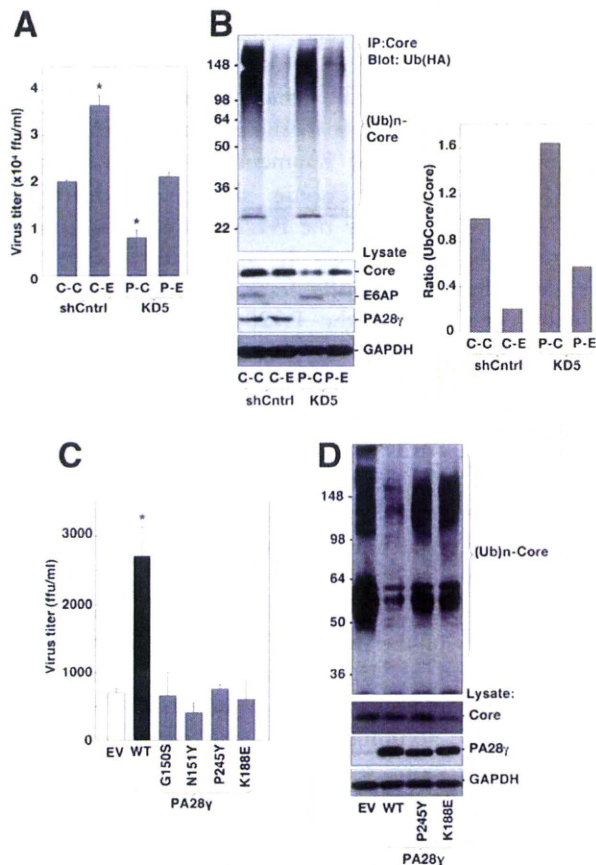


**Fig. 5.** PA28 $\gamma$  knockdown enhances E6AP-dependent ubiquitination of core protein and reduces virus titer. (A) shCntrl and KD5 cells transfected with plasmids encoding the negative control (C-C and P-C) or E6AP (C-E and P-E) shRNA were treated with puromycin for 2 days. The remaining cells seeded at  $2.5 \times 10^4$  cells in a 24-well plate were infected with the JFH-1 virus at an moi of 0.05, and infectious virus titers in the supernatants were determined at 72 hours postinfection by way of focus-forming assay. (B) The cells transfected and infected as in (A) were further transfected with a plasmid encoding HA-tagged ubiquitin at 48 hours postinfection. The cells were treated with 10  $\mu$ M MG132 for 5 hours at 72 hours postinfection and subjected to immunoprecipitation with anti-core monoclonal antibody and immunoblotting with anti-HA antibody. The ratio of ubiquitination of HCV core protein was assessed by the densitometries of the ubiquitinated and unubiquitinated core proteins. (C) KD5 cells transfected with plasmids encoding wild-type or mutant PA28 $\gamma$ ; were infected with the JFH-1 virus at an moi of 0.05 at 24 hours posttransfection, and the infectious titers in the supernatant were determined at 72 hours postinfection by way of focus-forming assay. (D) KD5 cells transfected with plasmids encoding HCV core protein and HA-tagged ubiquitin, together with wild-type or mutant PA28 $\gamma$ ; were treated with 10  $\mu$ M MG132 for 5 hours at 24 hours posttransfection and subjected to immunoprecipitation with anti-core monoclonal antibody and immunoblotting with anti-HA antibody. EV, empty vector; WT, plasmid encoding wild-type PA28 $\gamma$ ; \* $P < 0.05$  versus shCntrl or KD5 cells transfected with the negative control or empty vector. Data are representative of three independent experiments.

control cells transfected with the plasmid encoding control shRNA (Fig. 5A [C-C]). Furthermore, the impaired virus production in the PA28 $\gamma$  knockdown

cells (KD5) was restored by the transfection of the plasmid encoding shRNA to E6AP (Fig. 5A [P-E]). Cells expressing hemagglutinin (HA)-tagged ubiquitin infected with the JFH-1 virus were immunoprecipitated by the anti-core antibody, and the immunoprecipitates were analyzed by immunoblotting with anti-HA antibody (Fig. 5B). E6AP knockdown decreased the ratio of ubiquitination of HCV core protein, in contrast to the increase of that by PA28 $\gamma$  knockdown (Fig. 5B, lanes C-E and P-C). Furthermore, E6AP knockdown in the PA28 $\gamma$  knockdown cells restored the ubiquitination of the core protein to a certain extent (Fig. 5B, lane P-E). It was shown that Pro<sup>245</sup> of PA28 $\gamma$  is critical for binding to the 20S proteasome, and that Gly<sup>150</sup> and Asn<sup>151</sup> of PA28 $\gamma$  are important for activation of the proteasome.<sup>26</sup> To further examine the functional significance of PA28 $\gamma$  on HCV propagation, expression plasmids encoding siRNA-resistant PA28 $\gamma$  mutants in which Gly<sup>150</sup>, Asn<sup>151</sup>, and Pro<sup>245</sup> were replaced with Ser (G150S), Tyr (N151Y), and Tyr (P245Y), respectively, were transfected into KD5 cells and inoculated with JFH-1 virus at 24 hours posttransfection. The infectious virus titers in the culture supernatant were determined at 3 days postinfection (Fig. 5C). KD5 cells transfected with the plasmid encoding wild-type PA28 $\gamma$  exhibited a partial recovery of virus production, although those transfected with the plasmid encoding PA28 $\gamma$  G150S, N151Y, or P245Y or with an empty vector exhibited no effect on virus production. Replacing Lys<sup>188</sup> with Glu in PA28 $\gamma$  (PA28 $\gamma$  K188E) confers the capability of proteasome-mediated cleavage after hydrophobic, acidic, and basic residues such as those exhibited by PA28 $\gamma$ .<sup>27</sup> Expression of siRNA-resistant PA28 $\gamma$  K188E in KD5 cells could not restore virus production (Fig. 5D). The ubiquitination of HCV core protein was inhibited by expression of the wild-type PA28 $\gamma$  but not expression of the PA28 $\gamma$  mutants (P245Y or K188E) in KD5 cells (Fig. 5D). Collectively, these results suggest that PA28 $\gamma$  positively regulates HCV propagation by inhibiting degradation of HCV core protein by an E6AP/ubiquitin-dependent proteasome.

## Discussion

To explore the role of PA28 $\gamma$  on the life cycle of HCV, we examined the effects of knockdown of PA28 $\gamma$  in Huh7OK1 cells infected with the JFH-1 virus. Knockdown of PA28 $\gamma$  in Huh7OK1 cells before or after infection with the JFH-1 virus impaired



production of infectious particles but did not impair viral RNA replication. However, PA28 $\gamma$  knockdown did not affect the production of JEV, of which the capsid protein does not interact with PA28 $\gamma$ , suggesting that PA28 $\gamma$  knockdown does not affect the general sorting pathway of flavivirus. These results suggest that PA28 $\gamma$  is specifically involved in the postreplication steps of HCV life cycle. Our previous report indicated that HCV core protein was accumulated in the nucleus of the hepatocytes of HCV core transgenic/PA28 $\gamma$  knockout mice.<sup>8</sup> PA28 $\gamma$  is located mainly in the nucleus, although a small portion is also located in the cytoplasm<sup>7,28</sup> and can up-regulate trypsin-like proteasome activity, which cleaves after basic amino acid residues.<sup>27</sup> Previous studies have shown that some fraction of HCV core protein is translocated into the nucleus and quickly degraded in the PA28 $\gamma$ -dependent proteasome pathway.<sup>7,8,29</sup> Miyanari et al.<sup>30</sup> demonstrated that the core protein is localized on the surface of lipid droplets and is surrounded by nonstructural proteins, suggesting that HCV particles are assembled near the surface of the lipid droplets. In the present experiments, although HCV core protein was detected on the surface of the lipid droplets in both control and PA28 $\gamma$  knockdown cell lines, it was partially localized in the nucleus in PA28 $\gamma$  knockdown cells but not control cells. Furthermore, localization of HCV core protein on the surface of lipid droplets was impaired in PA28 $\gamma$  knockdown cells (Fig. 4). These results suggest that HCV core protein is partially translocated into the nucleus and degraded in the PA28 $\gamma$ -dependent proteasome pathway in HCV-infected cells and that PA28 $\gamma$  does not directly participate in the particle formation of HCV.

HCV core protein is degraded by at least two proteasome pathways: a ubiquitin-dependent pathway and a ubiquitin-independent and PA28 $\gamma$ -dependent pathway.<sup>17</sup> The E3 ligase E6AP catalyzes ubiquitin ligation to HCV core protein, resulting in enhanced degradation of the core protein in the cytoplasm.<sup>18</sup> Knockdown of E6AP up-regulated virus production in cells infected with the JFH-1 virus,<sup>18</sup> suggesting that E6AP/ubiquitin-dependent degradation of the core protein contributes to an antiviral response. In contrast, knockdown of PA28 $\gamma$  induced up-regulation of the ubiquitination of HCV core protein and down-regulation of the viral production, suggesting that PA28 $\gamma$ -dependent proteasome activity contributes to the proviral response by suppressing E6AP-dependent degradation of the core protein, thereby enhancing viral particle formation. The wild-type PA28 $\gamma$  enhances the trypsin-like activity of proteasome that cleaves peptide bonds

after basic residues of the substrates, whereas the PA28 $\gamma$  K188E mutant enhances the proteasome activity that cleaves peptide bonds after hydrophobic, acidic, and basic residues in the manner of PA28 $\alpha$ .<sup>27</sup> Therefore, the sizes of fragments produced by the PA28 $\gamma$ -dependent proteasome should be different from those produced by the PA28 $\alpha/\beta$ - or ubiquitination-mediated proteasome. It might be feasible to speculate that the peptide fragments of HCV core protein generated by the PA28 $\gamma$ -dependent proteasome or PA28 $\gamma$  *per se* may be directly or indirectly involved in the suppression of the E6AP-dependent ubiquitination of the core protein. Further studies will be needed to clarify the relationship between E6AP and PA28 $\gamma$  in the degradation and ubiquitination of HCV core protein. Figure 6 shows a schematic diagram of our hypothesis of the regulation of HCV propagation by PA28 $\gamma$ .

HCV core protein was found in not only nuclei but also cytoplasm of the infected KD5 cells (Fig. 4). The down-regulation of virus production should potentially reduce a total amount of the core protein in KD5 cells before a clear accumulation of the core protein in nuclei. Furthermore, a small amount of PA28 $\gamma$  was found in the PA28 $\gamma$  knockdown cells, suggesting that E6AP-dependent degradation of HCV core protein is not potentially suppressed in the PA28 $\gamma$  knockdown cells. If HCV core protein is constitutively expressed under the PA28 $\gamma$  knockout cells regardless of an amount of infected virus, a clear accumulation of the core protein in nuclei should be found without cytoplasmic expression of the core protein under the PA28 $\gamma$  knockout condition. We reported previously that HCC and liver steatosis in mouse are induced by the HCV core protein in the presence, but not the absence, of PA28 $\gamma$ .<sup>8</sup> Although HCV core protein is predominantly detected in the cytoplasm of the liver cells of PA28 $\gamma^{+/+}$  mice,<sup>8,31</sup> HCV core protein was clearly accumulated in the nuclei, but clearly reduced in cytoplasm, of liver cells of PA28 $\gamma^{-/-}$  mouse.<sup>8</sup> In addition, ubiquitination of HCV core protein was increased by PA28 $\gamma$  knockdown in the 293T cell line.<sup>8</sup> These results and the data in Fig. 5 suggest that the suppression of PA28 $\gamma$  function enhances the E6AP-dependent degradation of HCV core protein. Hence, the reason there is no difference between PA28 $\gamma^{+/+}$  and PA28 $\gamma^{-/-}$  mice with respect to the amount of core protein may be due to the competitive regulation of the core protein by E6AP- and PA28 $\gamma$ -dependent degradation mechanisms. E6AP-dependent degradation of HCV core protein in cytoplasm may be enhanced *in vivo* under the PA28 $\gamma$  knockout condition.

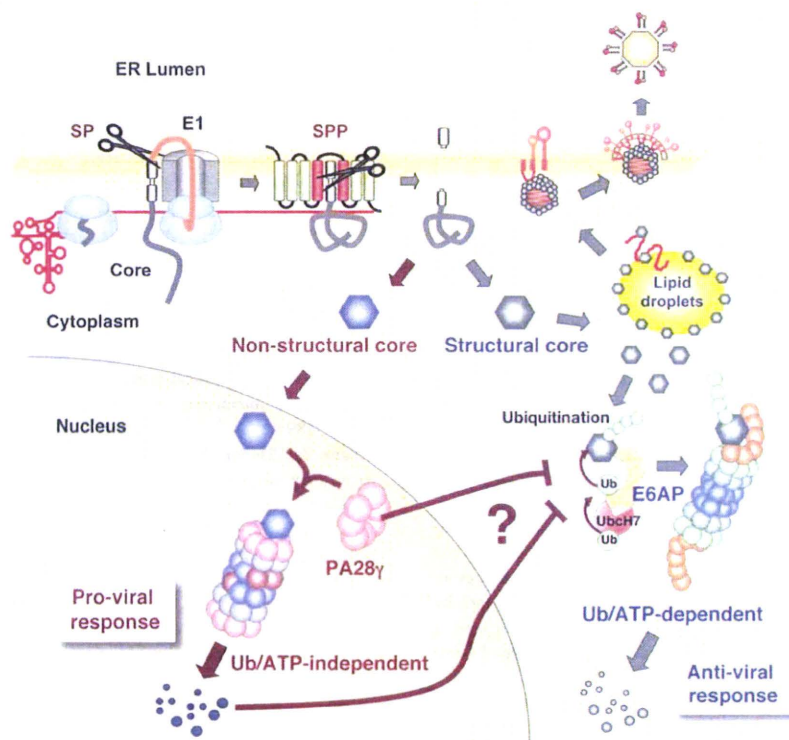


Fig. 6. Schematic diagram of the potential roles of PA28 $\gamma$  in HCV propagation. HCV core protein is cleaved off from the precursor polyprotein by signal peptidase (SP) and the signal sequence is further processed by signal peptide peptidase (SPP). The mature core protein mainly localizes on the lipid droplets close to the endoplasmic reticulum to form a nucleocapsid with the viral RNA genome and is incorporated into virus particles as a structural protein. In addition to the structural protein of HCV, the core protein has characteristics of a nonstructural protein. HCV core protein is degraded through ubiquitin-dependent and ubiquitin-independent proteasome pathways. E6AP catalyzes ubiquitin ligation to HCV core protein and promotes degradation in the cytoplasm, which contributes to the antiviral response. In contrast, the core protein partially migrates into the nucleus and is degraded through a ubiquitin-independent and PA28 $\gamma$ -dependent proteasome pathway, and the core protein fragments generated by the PA28 $\gamma$  pathway or PA28 $\gamma$  *per se* were suggested to participate in the suppression of E6AP-dependent ubiquitination of HCV core protein, which contributes to the proviral response.

In conclusion, in this study we demonstrated that the proteasome activator PA28 $\gamma$  positively regulates particle production of HCV by inhibiting E6AP-dependent ubiquitination of the core protein, in addition to our previous observation that PA28 $\gamma$  plays a crucial role in the development of liver pathology induced by HCV core protein.<sup>8</sup> PA28 $\gamma$  knockout mice exhibit only mild growth retardation.<sup>15,16</sup> Therefore, PA28 $\gamma$  may be a novel and promising antiviral target not only for elimination of HCV from hepatitis C patients but also for intervention in the progression of liver diseases induced by chronic HCV infection.

**Acknowledgment:** We thank H. Murase for her secretarial work. We also thank R. Bartenschlager and T. Wakita for providing cell lines and plasmids.

## References

1. Wasley A, Alter MJ. Epidemiology of hepatitis C: geographic differences and temporal trends. *Semin Liver Dis* 2000;20:1-16.
2. Moriishi K, Matsuura Y. Host factors involved in the replication of hepatitis C virus. *Rev Med Virol* 2007;17:343-354.
3. Hussy P, Langen H, Mous J, Jacobsen H. Hepatitis C virus core protein: carboxy-terminal boundaries of two processed species suggest cleavage by a signal peptide peptidase. *Virology* 1996;224:93-104.
4. Okamoto K, Mori Y, Komoda Y, Okamoto T, Okochi M, Takeda M, et al. Intramembrane processing by signal peptide peptidase regulates the membrane localization of hepatitis C virus core protein and viral propagation. *J Virol* 2008;82:8349-8361.
5. Barba G, Harper F, Harada T, Kohara M, Goulinet S, Matsuura Y, et al. Hepatitis C virus core protein shows a cytoplasmic localization and associates to cellular lipid storage droplets. *Proc Natl Acad Sci U S A* 1997;94:1200-1205.
6. Moriya K, Yotsuyanagi H, Shintani Y, Fujie H, Ishibashi K, Matsuura Y, et al. Hepatitis C virus core protein induces hepatic steatosis in transgenic mice. *J Gen Virol* 1997;78:1527-1531.
7. Moriishi K, Okabayashi T, Nakai K, Moriya K, Koike K, Murata S, et al. Proteasome activator PA28 $\gamma$ -dependent nuclear retention and degradation of hepatitis C virus core protein. *J Virol* 2003;77:10237-10249.
8. Moriishi K, Mochizuki R, Moriya K, Miyamoto H, Mori Y, Abe T, et al. Critical role of PA28 $\gamma$  in hepatitis C virus-associated steatogenesis and hepatocarcinogenesis. *Proc Natl Acad Sci U S A* 2007;104:1661-1666.
9. Miyamoto H, Moriishi K, Moriya K, Murata S, Tanaka K, Suzuki T, et al. Involvement of PA28 $\gamma$ -dependent pathway in insulin resistance induced by hepatitis C virus core protein. *J Virol* 2007;81:1727-1735.

10. Li X, Lonard D, Jung SY, Malovannaya A, Feng Q, Qin J, et al. The SRC-3/AIB1 coactivator is degraded in a ubiquitin- and ATP-independent manner by the REGgamma proteasome. *Cell* 2006;124:381-392.
11. Zhang Z, Zhang R. Proteasome activator PA28 gamma regulates p53 by enhancing its MDM2-mediated degradation. *EMBO J* 2008;27:852-864.
12. Chen X, Barton LF, Chi Y, Clurman BE, Roberts JM. Ubiquitin-independent degradation of cell-cycle inhibitors by the REGgamma proteasome. *Mol Cell* 2007;26:843-852.
13. Li X, Amazit L, Long W, Lonard DM, Monaco JJ, O'Malley BW. Ubiquitin- and ATP-independent proteolytic turnover of p21 by the REGgamma-proteasome pathway. *Mol Cell* 2007;26:831-842.
14. Jarriel-Encontre I, Bossis G, Piechaczyk M. Ubiquitin-independent degradation of proteins by the proteasome. *Biochim Biophys Acta* 2008;1786:153-177.
15. Barton LF, Runnels HA, Schell TD, Cho Y, Gibbons R, Tevethia SS, et al. Immune defects in 28-kDa proteasome activator gamma-deficient mice. *J Immunol* 2004;172:3948-3954.
16. Murata S, Kawahara H, Tohma S, Yamamoto K, Kasahara M, Nabeshima Y, et al. Growth retardation in mice lacking the proteasome activator PA28gamma. *J Biol Chem* 1999;274:38211-38215.
17. Suzuki R, Moriishi K, Fukuda K, Shirakura M, Ishii K, Shoji I, et al. Proteasomal turnover of hepatitis C virus core protein is regulated by two distinct mechanisms: a ubiquitin-dependent mechanism and a ubiquitin-independent but PA28gamma-dependent mechanism. *J Virol* 2009;83:2389-2392.
18. Shirakura M, Murakami K, Ichimura T, Suzuki R, Shimoji T, Fukuda K, et al. E6AP ubiquitin ligase mediates ubiquitylation and degradation of hepatitis C virus core protein. *J Virol* 2007;81:1174-1185.
19. Aoyagi K, Ohue C, Iida K, Kimura T, Tanaka E, Kiyosawa K, et al. Development of a simple and highly sensitive enzyme immunoassay for hepatitis C virus core antigen. *J Clin Microbiol* 1999;37:1802-1808.
20. Lohmann V, Korner F, Koch J, Herian U, Theilmann L, Bartenschlager R. Replication of subgenomic hepatitis C virus RNAs in a hepatoma cell line. *Science* 1999;285:110-113.
21. Wakita T, Pietschmann T, Kato T, Date T, Miyamoto M, Zhao Z, et al. Production of infectious hepatitis C virus in tissue culture from a cloned viral genome. *Nat Med* 2005;11:791-796.
22. Pietschmann T, Lohmann V, Kaul A, Krieger N, Rinck G, Rutter G, et al. Persistent and transient replication of full-length hepatitis C virus genomes in cell culture. *J Virol* 2002;76:4008-4021.
23. Mori Y, Okabayashi T, Yamashita T, Zhao Z, Wakita T, Yasui K, et al. Nuclear localization of Japanese encephalitis virus core protein enhances viral replication. *J Virol* 2005;79:3448-3458.
24. Targett-Adams P, Chambers D, Gledhill S, Hope RG, Coy JF, Girod A, et al. Live cell analysis and targeting of the lipid droplet-binding adipocyte differentiation-related protein. *J Biol Chem* 2003;278:15998-16007.
25. Okamoto T, Omori H, Kaname Y, Abe T, Nishimura Y, Suzuki T, et al. A single-amino-acid mutation in hepatitis C virus NS5A disrupting FKBP8 interaction impairs viral replication. *J Virol* 2008;82:3480-3489.
26. Zhang Z, Clawson A, Realini C, Jensen CC, Knowlton JR, Hill CP, et al. Identification of an activation region in the proteasome activator REGalpha. *Proc Natl Acad Sci U S A* 1998;95:2807-2811.
27. Li J, Gao X, Ortega J, Nazif T, Joss L, Bogvo M, et al. Lysine 188 substitutions convert the pattern of proteasome activation by REGgamma to that of REGs alpha and beta. *EMBO J* 2001;20:3359-3369.
28. Nikaïdo T, Shimada K, Nishida Y, Lee RS, Pardee AB, Nishizuka Y. Loss in transformed cells of cell cycle regulation of expression of a nuclear protein recognized by SLE patient antisera. *Exp Cell Res* 1989;182:284-289.
29. Suzuki R, Sakamoto S, Tsutsumi T, Rikimaru A, Tanaka K, Shimoike T, et al. Molecular determinants for subcellular localization of hepatitis C virus core protein. *J Virol* 2005;79:1271-1281.
30. Miyanari Y, Atsuzawa K, Usuda N, Watashi K, Hishiki T, Zayas M, et al. The lipid droplet is an important organelle for hepatitis C virus production. *Nat Cell Biol* 2007;9:1089-1097.
31. Moriya K, Fujie H, Shintani Y, Yotsuyanagi H, Tsutsumi T, Ishibashi K, et al. The core protein of hepatitis C virus induces hepatocellular carcinoma in transgenic mice. *Nat Med* 1998;4:1065-1067.

## Involvement of Ceramide in the Propagation of Japanese Encephalitis Virus<sup>†</sup>

Hideki Tani, Mai Shiokawa, Yuuki Kaname, Hiroto Kambara, Yoshio Mori,  
Takayuki Abe, Kohji Moriishi, and Yoshiharu Matsuura\*

Department of Molecular Virology, Research Institute for Microbial Diseases, Osaka University, Osaka, Japan

Received 27 November 2009/Accepted 22 December 2009

**Japanese encephalitis virus (JEV) is a mosquito-borne RNA virus and one of the most important flaviviruses in the medical and veterinary fields. Although cholesterol has been shown to participate in both the entry and replication steps of JEV, the mechanisms of infection, including the cellular receptors of JEV, remain largely unknown. To clarify the infection mechanisms of JEV, we generated pseudotype (JEVpv) and recombinant (JEVrv) vesicular stomatitis viruses bearing the JEV envelope protein. Both JEVpv and JEVrv exhibited high infectivity for the target cells, and JEVrv was able to propagate and form foci as did authentic JEV. Anti-JEV envelope antibodies neutralized infection of the viruses. Treatment of cells with inhibitors for vacuolar ATPase and clathrin-mediated endocytosis reduced the infectivity of JEVpv, suggesting that JEVpv enters cells via pH- and clathrin-dependent endocytic pathways. Although treatment of the particles of JEVpv, JEVrv, and JEV with cholesterol drastically reduced the infectivity as previously reported, depletion of cholesterol from the particles by treatment with methyl  $\beta$ -cyclodextrin enhanced infectivity. Furthermore, treatment of cells with sphingomyelinase (SMase), which hydrolyzes membrane-bound sphingomyelin to ceramide, drastically enhanced infection with JEVpv and propagation of JEVrv, and these enhancements were inhibited by treatment with an SMase inhibitor or C<sub>6</sub>-ceramide. These results suggest that ceramide plays crucial roles in not only entry but also egress processes of JEV, and they should assist in the clarification of JEV propagation and the development of novel therapeutics against diseases caused by infection with flaviviruses.**

*Japanese encephalitis virus (JEV)* is a small, enveloped virus belonging to the family *Flaviviridae* and the genus *Flavivirus*, which also includes *Dengue virus (DENV)*, *West Nile virus (WNV)*, *Yellow fever virus*, and *Tick-borne encephalitis virus (TBEV)*. JEV is the most common agent of viral encephalitis, causing approximately 50,000 cases annually, of which 15,000 will die, and up to 50% of survivors are left with severe residual neurological complications. JEV has a single-stranded positive-sense RNA genome of approximately 11 kb, encoding a single large polyprotein, which is cleaved by the host- and virus-encoded proteases into three structural proteins, capsid (C), premembrane (PrM), and envelope (E), and seven non-structural proteins. The structural proteins are components of viral particles, and the E protein is suggested to interact with a cell surface receptor molecule(s). Although a number of cellular components, including heat shock cognate protein 70 (33), glycosaminoglycans, such as heparin or heparan sulfate (21, 41), and laminin (3), have been shown to participate in JEV infection, the precise mechanisms by which these receptor candidates participate in JEV infection remain largely unclear.

In addition to the many studies identifying and characterizing receptor molecules in numerous viruses, data suggesting the involvement of membrane lipids, such as sphingolipids and cholesterol, in viral infection have also been accumulating. Lipid rafts consisting of sphingolipids and cholesterol and distributing to the outer leaflet of the cell membrane have been shown to be involved in the infection of not only many viruses

but also several bacteria and parasites (24), in addition to playing roles in various functions such as lipid sorting, protein trafficking (26, 47), cell polarity, and signal transduction (38). With respect to cholesterol itself, various aspects of the life cycle of flaviviruses have been shown to involve this lipid, including the entry of DENV (34), hepatitis C virus (HCV) (16), and WNV (27), the membrane fusion of tick-borne encephalitis virus (40), and the replication of HCV (14, 17), WNV (23), and DENV (35). Recently Lee et al. (20) showed that treatment with cholesterol efficiently impairs both the entry and replication steps of JEV and DENV-2 but enhances infection with the Sindbis virus (22).

On the other hand, sphingolipids, including sphingomyelins and glycosphingolipids, are ubiquitous components of eukaryotic cell membrane structures, providing integrity to cellular membranes. Ceramide is one of the intermediates of sphingolipids and plays roles in cell differentiation, regulation of apoptosis and protein secretion, induction of cellular senescence, and other processes (2). Ceramide is generated from the hydrolysis of sphingomyelin by sphingomyelinase (SMase) or from catalysis by serine-palmitoyl-coenzyme A (CoA) transferase and ceramide synthase. Ceramide spontaneously self-associates to form ceramide-enriched microdomains and then to form larger ceramide-enriched membrane platforms which serve as the spatial and temporal organization for cellular signalosomes and for regulation of protein functions (2). The ceramide-enriched platforms have also been used by many pathogens to facilitate entry and infection (2). The acid SMase is activated not only by multiple stimuli, including receptor molecules, gamma irradiation, and some chemicals, but also by infection with some bacteria or viruses (36). Rhinovirus activates the SMase for generation of ceramide and forms ceramide-enriched membrane platforms that serve in the infection of

\* Corresponding author. Mailing address: Department of Molecular Virology, Research Institute for Microbial Diseases, Osaka University, 3-1 Yamada-oka, Suita, Osaka 565-0871, Japan. Phone: 81-6-6879-8340. Fax: 81-6-6879-8269. E-mail: matsuura@biken.osaka-u.ac.jp.

<sup>†</sup> Published ahead of print on 6 January 2010.